Statistical analysis

Statistical comparisons of mean final tumor volumes in the xenograft studies were made using a one-way analysis of variance (ANOVA). $P<0.05$ was considered statistically significant.

Results

Classification of endometrial cancer cells according to the mutational status of *PIK3CA*, *PTEN*, and *K-Ras*

We previously reported copy number losses for *PTEN* (26%) and gains for *PIK3CA* (19%) and *K-Ras* (13%) in our 31 clinical samples, in addition to mutations of *K-Ras*, *PTEN*, *PIK3CA*, and *AKT1* [8,9,25]. We confirmed that all 13 endometrial cancer cell lines possess one or more alterations (mutations and/or copy number alterations) in the *PIK3CA*, *PTEN*, and *K-Ras* genes (Table 1, Figure 1A and 1B). *AKT1* mutations were not detected in these 13 cell lines. We classified 13 endometrial cancer cell lines into 4 groups according to the mutational status of *PIK3CA*, *PTEN*, and *K-Ras* (Table 1): group A (n = 4), with coexistent mutations of *PIK3CA* and *PTEN*; group B (n = 5), with *PTEN* mutation alone; group C (n = 2), with coexistent mutations of *K-Ras* and *PIK3CA*; and group D (n = 2), with copy number gain of *K-Ras* (without any mutations in these 3 genes). We previously reported that PTEN expression was not detected in *PTEN* mutant endometrial cancer cell lines [8]. We have found no endometrial cell lines without any alterations in the Ras-PI3K pathway, suggesting that this pathway is essentially activated in the majority of endometrial cancer cell lines.

Mutations in *PIK3CA* and/or *PTEN*, in the absence of mutations in *K-Ras*, define the antiproliferative response to NVP-BEZ235 and RAD001 in endometrial cancer cell lines

We performed MTT (Methyl thiazolyl tetrazorium) assay by NVP-BEZ235 and RAD001 in the 13 endometrial cell lines. RAD001 (100 nM) showed a growth inhibitory effect against 10 of the 13 cell lines (including all 9 group A and B cell lines), with a 30–70% reduction in cells (Figure 2A–2D). NVP-BEZ235 (100 nM) inhibited cell growth, with a 30–90% reduction in all 13 cell lines. The IC_{50} values for cell proliferation by RAD001 were greater than 100 nM (non-sensitive) in 6 out of the 9 cell lines in groups A and B, whereas the IC_{50} values for NVP-BEZ235 were less than 100 nM (sensitive) in all 9 cell lines in groups A and B (Table 1). Dose-dependent growth suppression was more clearly induced by NVP-BEZ235 than by RAD001 in 8 of the 9 cell lines in groups A and B (Figure 2A–2D). The IC_{50} values for all 4 cell lines in groups C and D were greater than 100 nM for NVP-BEZ235 (Table 1). Taken together, these data show that the existence of *PTEN* and/or *PIK3CA* mutations without *K-Ras* mutations is associated with sensitivity to NVP-BEZ235. In addition, high-dose NVP-BEZ235 might be more broadly effective than RAD001 for treatment of endometrial carcinomas. Growth curves of all cell lines in 1 graph were available for both NVP-BEZ235 and RAD001, respectively (Figures S1 and S2).

NVP-BEZ235 suppresses phosphorylation of Akt, GSK3beta, S6, and 4EBP1, whereas RAD001 suppresses phosphorylation of S6 and 4EBP1

We performed immunoblotting with lysates prepared from cells treated with NVP-BEZ235 or RAD001. The phosphorylation (p-) levels of 4E-BP1 and S6 were clearly suppressed by both inhibitors at low concentrations (0.625–2.5 nM). NVP-BEZ235 also suppressed the level of p-Akt (Ser473 and Thr308) (50–1000 nM) in these cells (Figure 3A and 3B). RAD001 did not suppress the phosphorylation level of Akt at any dose (Figure 3A and 3B). The dose dependency of the phosphorylation levels of mTORC1-dependent proteins (4E-BP1 and S6) and Akt suggests that NVP-BEZ mainly works as an mTOR (mTORC1) inhibitor at lower concentrations and functions as a dual PI3K/mTOR inhibitor at higher concentrations.

Next, we performed time-course experiments with NVP-BEZ235 and RAD001. Long-term exposure to NVP-BEZ235 (250 nM) resulted in sustained inhibition of p-S6 and p-4E-BP1. However, the phosphorylation levels of Akt and GSK3beta (an mTORC1-independent protein) recovered nearly to the baseline levels within 24 h (Figure 3C). Exposure to RAD001 resulted in a drastic reduction in the level of p-4EBP1 in 15 min, but the level

Table 1. Classification of endometrial cancer cell lines by mutational status and IC50 values to NVP-BEZ235 and RAD001.

Group	Cell line	Mutational status			Copy number alterations			IC_{50} (nM)	
		PIK3CA	*PTEN* (mutated exons)	*K-Ras*	*PIK3CA*	*PTEN*	*K-Ras*	BEZ235	RAD001
A	HEC-116	Mut (R88Q)	Mut 6(M), 7(N)	wild type	nl	nl	nl	19	6
	HEC-6	Mut (R108H)	Mut 4(F), 8(F)	wild type	nl	nl	nl	19	400
	HEC-59	Mut (R38C)	Mut 2(M), 7(N), 7(M), 7(F)	wild type	nl	nl	nl	24	220
	HEC-88	Mut (E365K)	Mut 5(M), 6(M), 8(M), 8(M)	wild type	nl	nl	nl	44	440
B	AN3CA	wild type	Mut 5(N)	wild type	nl	nl	nl	20	14
	Ishikawa	wild type	Mut 8(F), 8(F)	wild type	Gain	nl	nl	30	50
	HEC-151	wild type	Mut 2(M), 4(F)	wild type	nl	nl	nl	51	130
	HEC-108	wild type	Mut 1(F), 8(F)	wild type	nl	nl	nl	55	730
	RL95	wild type	Mut 8(F), 8(F)	wild type	nl	nl	nl	90	>1000
C	HEC-1B	Mut (G1049R)	wild type	Mut (G12D)	Gain	nl	nl	220	200
	HHUA	Mut (R88Q)	Mut 5(F), 8(F)	Mut (G12V)	nl	nl	nl	250	>1000
D	KLE	wild type	wild type	wild type	nl	nl	Gain	110	>1000
	HEC-50B	wild type	wild type	wild type	Gain	nl	Gain	100	>1000

(M) Missense mutation, (N) Non-sense mutation, (F) Frameshift mutation.

doi:10.1371/journal.pone.0037431.t001

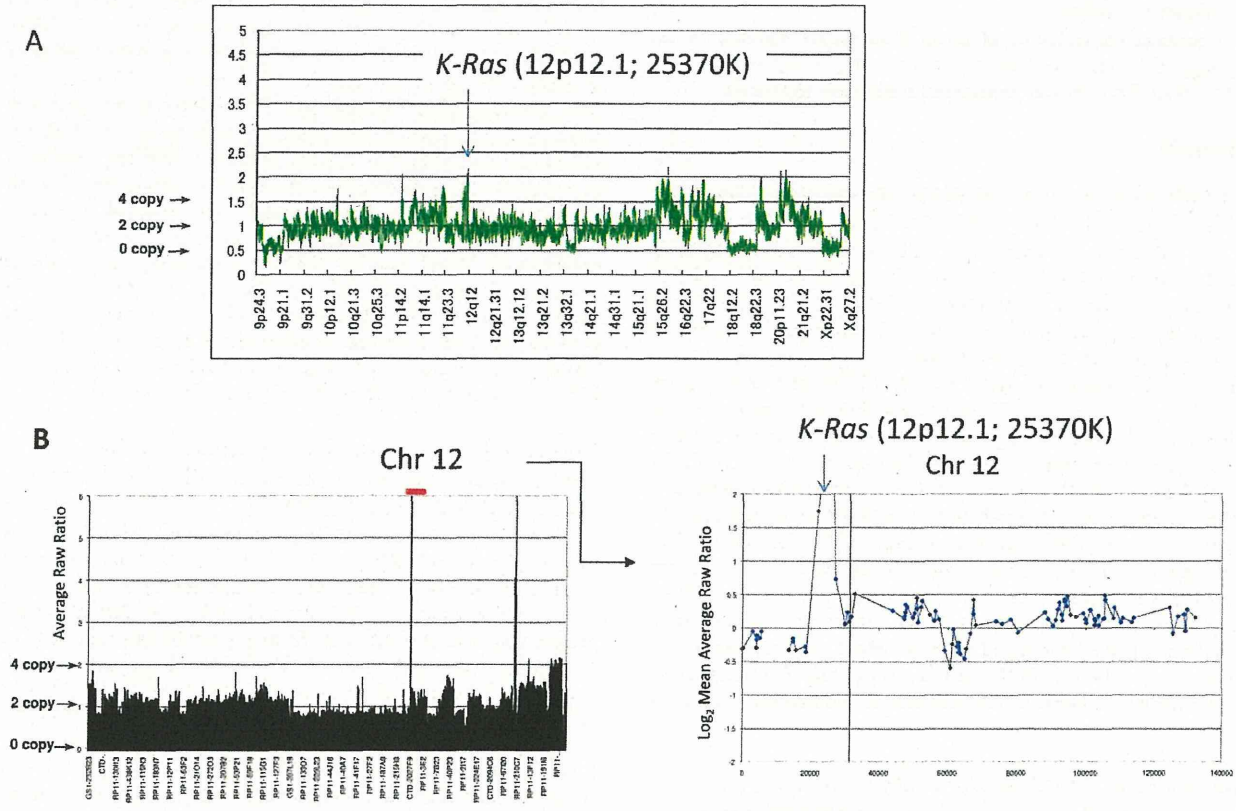

Figure 1. Copy number gain at the locus of *K-Ras* (12p12.1) in the two group D cell lines. (A) SNP array 'karyograms' (250K) of HEC-50B cells. The graph shows the total copy number through chromosome 9p-X. The locus of *K-Ras* is amplified as indicated. (B) Array CGH of KLE cells. The graphs show total copy number throughout the entire genome (Left) and chromosome 12 (Right). The locus of *K-Ras* is amplified as indicated.
doi:10.1371/journal.pone.0037431.g001

was recovered within 6 hours; the level of p-S6 was continuously suppressed over the time course (Figure 3C). We confirmed that the phosphorylation level of ERK was not affected by both RAD001 and NVP-BEZ235 (Figure 3A–3C).

NVP-BEZ235 robustly induces dose-dependent G1 arrest in "sensitive" cells

We conducted fluorescence-activated cell sorting (FACS)-based cell cycle analyses before and after NVP-BEZ235 or RAD001 treatment in a subset of the cell lines. At a low concentration (10 nM), G1 arrest was slightly induced by both RAD001 and NVP-BEZ235 (<15%) in group A and group B cell lines (Figure 4A–4D). At a higher concentration (100 nM), G1 arrest was much more effectively induced by NVP-BEZ235 than by RAD001 in three of the four cell lines (Figure 4A–4D). Dose-dependent G1 arrest by NVP-BEZ235 was confirmed in all the other group A and B cell lines (data not shown). G1 arrest was also observed to be induced by either RAD001 or NVP-BEZ235 in the 4 cell lines of groups C and D; however, the dose-dependent effect of NVP-BEZ235 was not significant, except for HEC-1B cells (Figure S3A–S3D). The sub-G1 population was not significantly induced by either inhibitor in all cell lines examined, suggesting that the antitumor effect of these inhibitors is predominantly cytostatic, not cytotoxic.

In vivo antitumor effect of NVP-BEZ235 and RAD001 in a mouse xenograft model

We examined in vivo antitumor activity of both NVP-BEZ235 and RAD001 in mice inoculated with either group A (HEC-59) or group B (AN3CA) cells. Both NVP-BEZ235 and RAD001 significantly suppressed the tumor growth of the xenografts, compared with the control (vehicle). No significant adverse effects, including a body weight loss of more than 10%, were observed in the examined mice (data not shown). Inconsistent with the in vitro data, the effects of NVP-BEZ235 and RAD001 were comparable (Figure 5A–5C).

We then evaluated the phosphorylation levels of the targeted molecules as pharmacodynamic markers. We extracted proteins from the second, third, and fourth largest tumors of each group. Although there were variations in the phosphorylation levels in the control group, NVP-BEZ235 suppressed the phosphorylation levels of Akt, FOXO1/3a, and S6 at 1 h. However, the phosphorylation levels of these proteins recovered to the baseline levels within 24 h (Figure 5D). RAD001 had clearly suppressed the p-S6 level at 1 h, and the effect partly remained at 24 h after the treatment (Figure 5D). Taken together with the in vitro experiments, these results indicate that the antitumor activity of NVP-BEZ235 might not be sufficiently maintained during treatment.

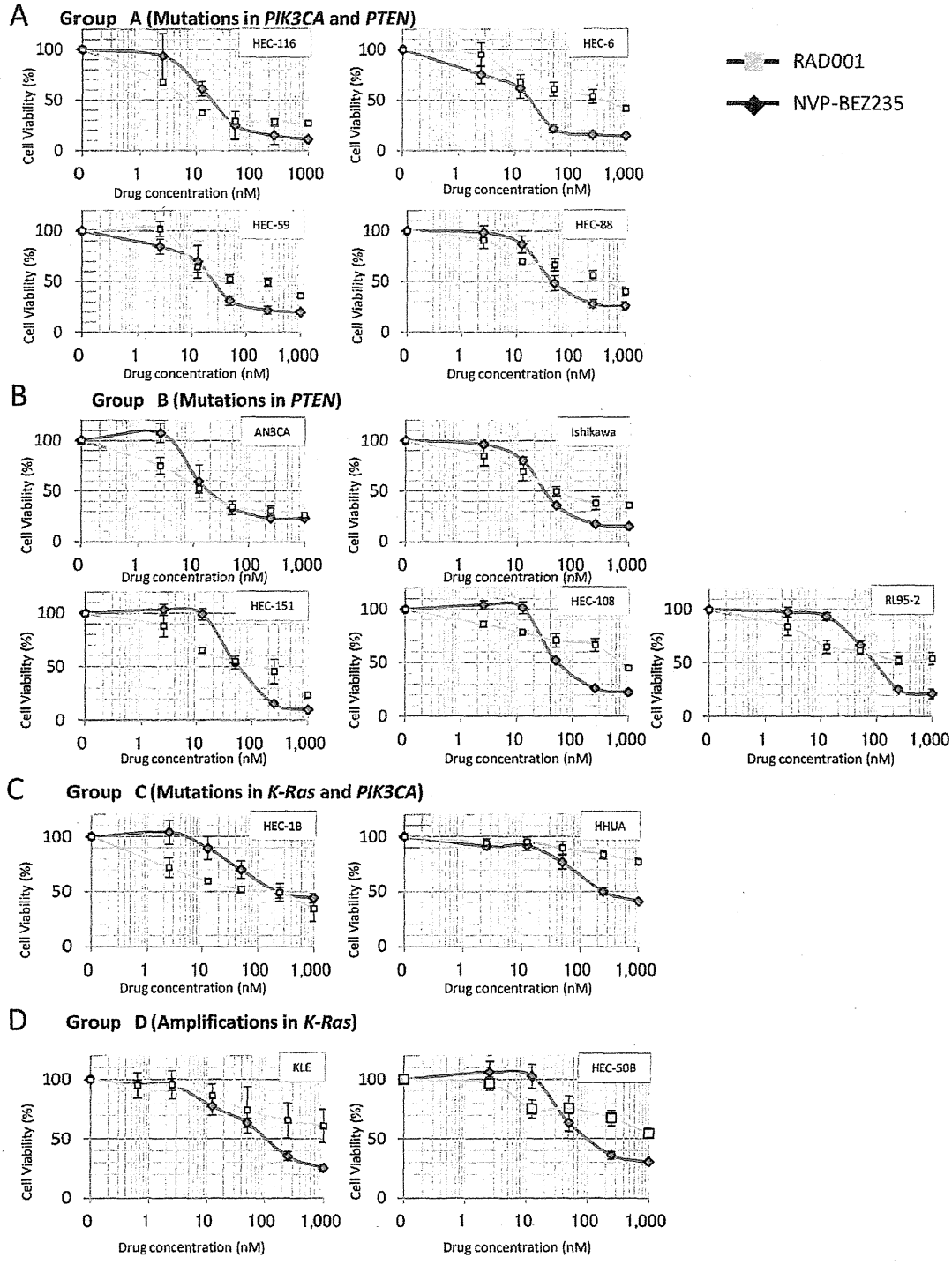

Figure 2. Inhibition of cell proliferation by NVP-BEZ235 and RAD001. (A)–(D) WST-8 assay showing the sensitivity of endometrial cancer cells to NVP-BEZ235 and RAD001 at increasing concentrations of drug (nmol/L) for 72 h. The data was normalized to the value of control cells. (A) Four group A cell lines with double mutations of *PIK3CA* and *PTEN*, (B) Five group B cell lines with *PTEN* mutations, (C) Two group C cell lines with coexistent mutations of *K-Ras* and *PIK3CA*, and (D) Two group D cell lines with chromosomal copy number amplification at the locus of *K-Ras*. All experiments were repeated 3 times, and each value is shown as the mean of 3 experiments ± S.D.
doi:10.1371/journal.pone.0037431.g002

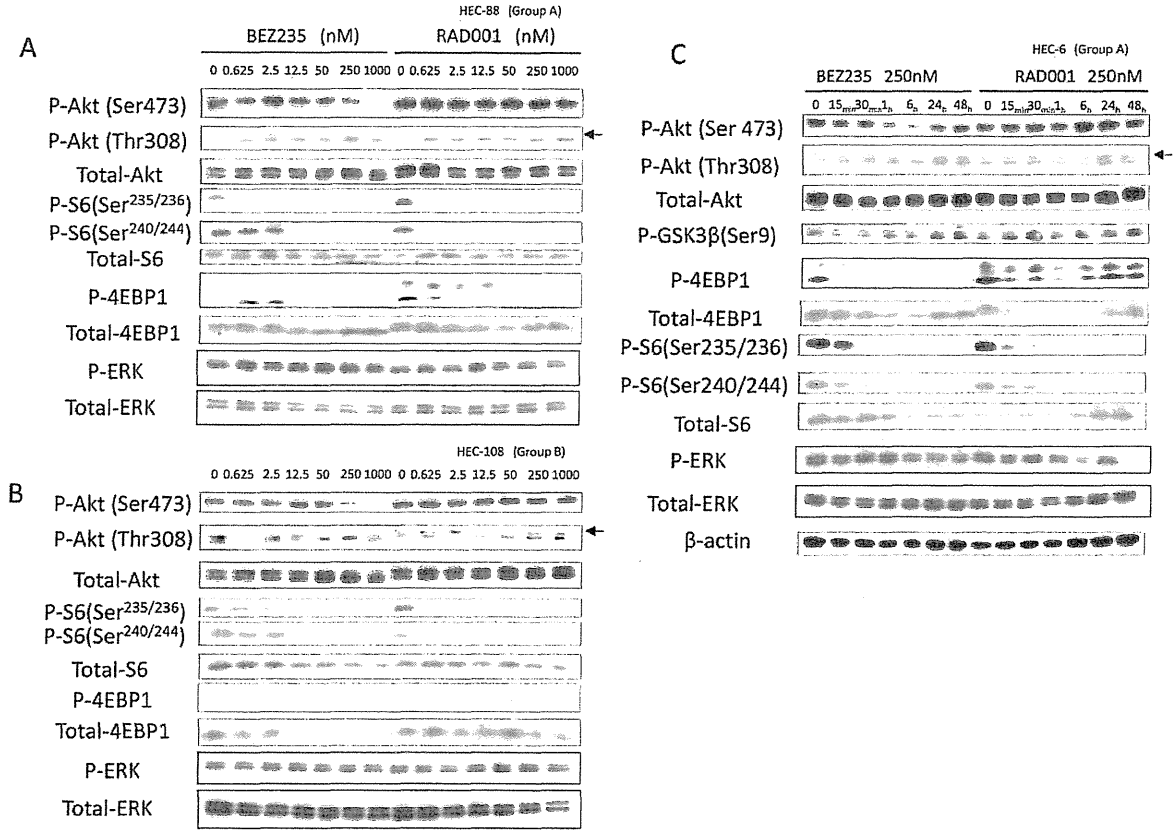

Figure 3. Inhibition of PI3K/mTOR signaling by NVP-BEZ235 and inhibition of mTOR signaling by RAD001 in endometrial cancer cell lines. (A)–(B) Western blot of total lysates of HEC-88 (group A) and HEC-108 (group B) cells, treated with NVP-BEZ235 or RAD001 at concentrations ranging from 0 to 1,000 nmol/L with 10% fetal bovine serum (FBS). phospho-Akt (Ser473, Thr308), phospho-S6 (Ser235/236, Ser240/244), and phospho-4EBP1 (Thr 37/46) levels are shown with total Akt level for a loading control. (C) Western blot of total lysates of HEC-6 (group A) cells treated with NVP-BEZ235 or RAD001 at a dose of 100 nM for up to 48 hours with 10% FBS. Phosphorylation levels of the PI3K/mTOR signaling are shown with loading controls.
doi:10.1371/journal.pone.0037431.g003

Inhibition of the MAPK pathway synergistically (or additively) suppresses cell proliferation and induces G1 arrest in *K-Ras* mutant endometrial cell lines

Because the 4 cell lines with *K-Ras* alterations (HEC-1B, HHUA, KLE, and HEC-50B) were less sensitive to both NVP-BEZ235 and RAD001, compared with *K-Ras* wild-type cells with *PTEN* mutations (groups A and B), we combined NVP-BEZ235 (or RAD001) with a MEK inhibitor (PD98059 or UO126) for use in these 4 cell lines (groups C and D). MTT assay revealed that PD98059 (50 μM) or UO126 (10 μM) alone showed a limited growth inhibitory effect with a 10–30% reduction in the 4 cell lines (Figure 6A and 6B, Figure S4A and S4B). However, after treatment with NVP-BEZ235 (250 nM) combined with PD98059 (20–50 μM) or UO126 (10 μM), cell proliferation was suppressed synergistically or additively with a 45–70% reduction (Figure 6A and 6B, Figure S4A and S4B). FACS analysis showed that G1 arrest was markedly induced by a combination of PD98059 (or UO126) and NVP-BEZ235 (Figure 6C and 6D, Figure S4C and S4D). In HEC-1B and HEC-50B cells, the G0/G1 ratio was significantly higher for the combination of PD98059 and NVP-BEZ235 than for either compound alone (Figure 6C and 6D). A similar synergistic effect was also observed with the combination of PD98059 (or UO126) and RAD001 (250 nM), although the effect of RAD001 was weaker than that of NVP-BEZ235 (Figure 6C and 6D, Figure S4C and S4D). The sub-G1 population was not significantly increased in groups C and D cells when using the combination of NVP-BEZ235 and a MEK inhibitor, PD98059 (<5%), as compared to that when using the control or NVP-BEZ235 alone.

Phosphorylation levels of Akt, S6, and ERK in cells with K-Ras alterations treated with RAD001, NVP-BEZ235, and PD98059

We analyzed the PI3K/mTOR and MAPK signaling pathways in cells of groups C and D by western blotting. NVP-BEZ235 at 250 nM suppressed the phosphorylation levels of AKT and S6 in HEC-1B, HEC-50B, and KLE cells. In HHUA cells, the total AKT level was slightly elevated, although the p-AKT level was not significantly changed by NVP-BEZ235 alone (Figure 7). RAD001 at 250 nM suppressed the p-S6 level in all cells of groups C and D (Figure 7). Both RAD001 and NVP-BEZ235 did not suppress the p-ERK level, whereas a MEK inhibitor, PD98059, decreased the p-ERK level in these cells.

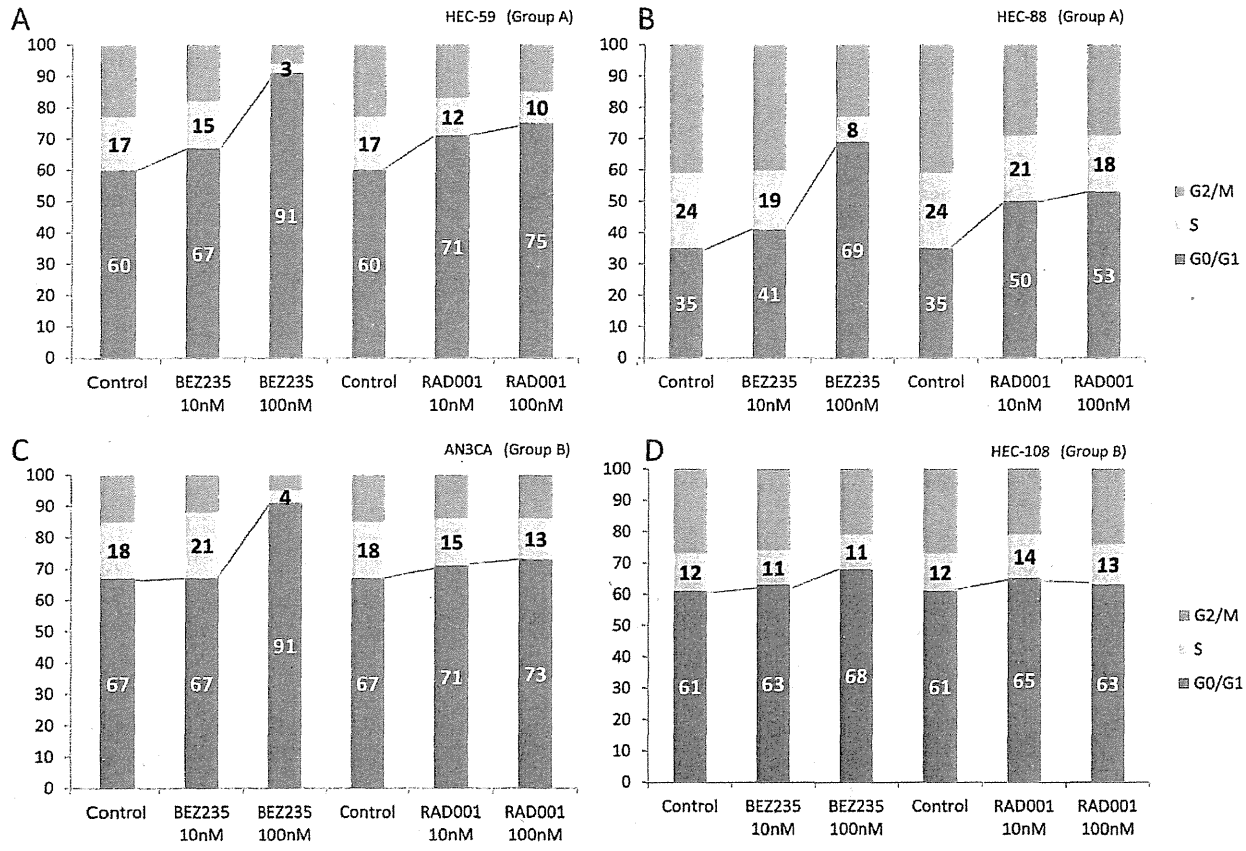

Figure 4. Flowcytometric analysis of cell cycle in cancer cells treated with either NVP-BEZ235 or RAD001. (A–D) Cells (5×10^5) were seeded in the presence of 10% serum and treated with NVP-BEZ235 or RAD001 for 48 h at a dose of 10 nM or 100 nM, respectively. A higher dose of NVP-BEZ235 (100 nM) significantly augmented the percentage of cells in the G0-G1phase of the cell cycle, compared with that of RAD001 (100 nM). (A)–(B); The data from two group A cells. (C)–(D); the data from two group B cells.
doi:10.1371/journal.pone.0037431.g004

Discussion

We examined activity of the PI3K/mTOR pathway inhibitors in endometrial cancer cell lines with a particular focus on (i) the antitumor effect of an mTOR inhibitor (RAD001) and a dual PI3K/mTOR inhibitor (NVP-BEZ235), (ii) predictive biomarkers of the mutational status of the PI3K pathway genes, and (iii) combined inhibition of the MAPK pathway and the PI3K/mTOR pathway in *K-Ras* mutant cells. MTT assay and FACS analysis in a panel of endometrial cancer cell lines revealed a clear dose-dependent effect of NVP-BEZ235 on cell proliferation. NVP-BEZ235 induces G1 arrest much more efficiently at a higher concentration (100 nM) than at a lower concentration (10 nM). In contrast, RAD001 does not show evidence of such dose dependency. Previous reports also suggested that NVP-BEZ235 was more effective than rapalogs at higher concentrations [26,27]. PI3K activity might not be sufficiently suppressed by 100 nM NVP-BEZ235, as indicated by the observation that decreased phosphorylation of Akt (Thr308) is not observed at 50 nM but is observed at 250 nM or higher. In addition, IC_{50} values were under 100 nM in cells from groups A and B. These data are in agreement with previous reports on other cancers that indicate a discrepancy between the basal activity of the PI3K/Akt pathway and the biochemical activity of NVP-BEZ235 [26–29]. Nevertheless, the dose-dependent antiproliferative activity at concentrations $\geq$250 nM suggests that the effect of NVP-BEZ235 was, at least in part, caused by inhibition of the PI3K/Akt pathway. Our data suggest that a dual inhibitor of PI3K/mTOR might be a more promising therapeutic strategy than a single mTOR inhibitor in endometrial cancer.

Our in vivo studies in 2 cell lines of xenograft mice support the in vitro findings that inhibition of the PI3K/mTOR axis has an antitumor effect in endometrial cancers. We did not see any superior efficacy of NVP-BEZ235 in the in vivo study. The concentrations we used were 40 mg/kg for NVP-BEZ235 and 5 mg/kg for RAD001, which are equivalent with the previous in-vivo experiments [26,28,30–32]. In a pharmacodynamic analysis, the levels of p-Akt, p-GSK3beta, p-FOXO1/3a, and p-S6 in tumors returned to the baseline levels within 24 h after administration of NVP-BEZ235, suggesting that inhibition of PI3K signaling by NVP-BEZ235 might not be sufficiently maintained over time. This is compatible with previous data showing that inhibition of p-Akt (Ser473) was maintained for 16 h, with recovery to baseline levels at 24 h [33]. It remains to be determined which oral dosing schedule is optimal in treatment of endometrial cancer. As well, the mechanisms of in-vivo antitumor effect by these drugs should be more clarified, as inhibition of mTOR might result in anti-angiogenic effect by suppressing HIF1-VEGF pathway [34].

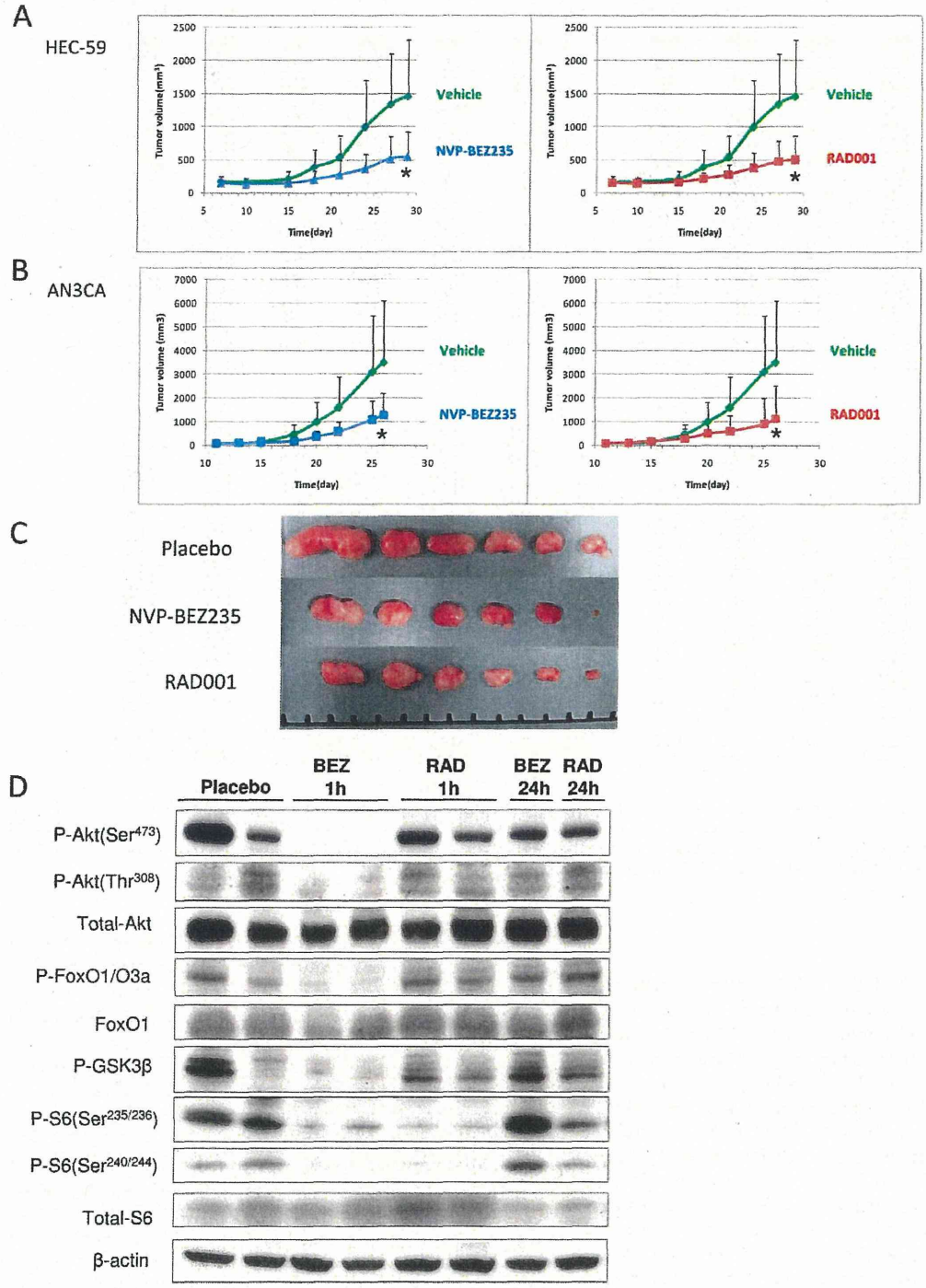

Figure 5. in vivo anti-tumor effect of NVP-BEZ235 and RAD001 in nude mice. Subcutaneous xenograft tumors in athymic BALB/c mice were established in the injection of endometrial carcinoma cells. Mice were treated with a daily dose of 40 mg/kg (NVP-BEZ235) or with a daily dose of 2.5 mg/kg RAD001 or vehicle alone (control). Each treatment group contained 6 mice; (A) HEC-59 and (B) AN3CA. Tumor volumes were calculated by the formula {(major axis)*(minor axis)2/2}mm3 twice a week. Groups were compared at the end of treatment. Points, mean; bars, SD, *;$p<0.05$. (C) Appearance of subcutaneous tumors in HEC-59 xenografts. (D) Western blot of total lysates from the HEC-59 xenografts. p-Akt, p-FOXO1/3a, p-GSK3beta, p-S6 were assessed 1 and 24 h after the last drug administration. Total Akt and beta-actin were shown as loading controls.
doi:10.1371/journal.pone.0037431.g005

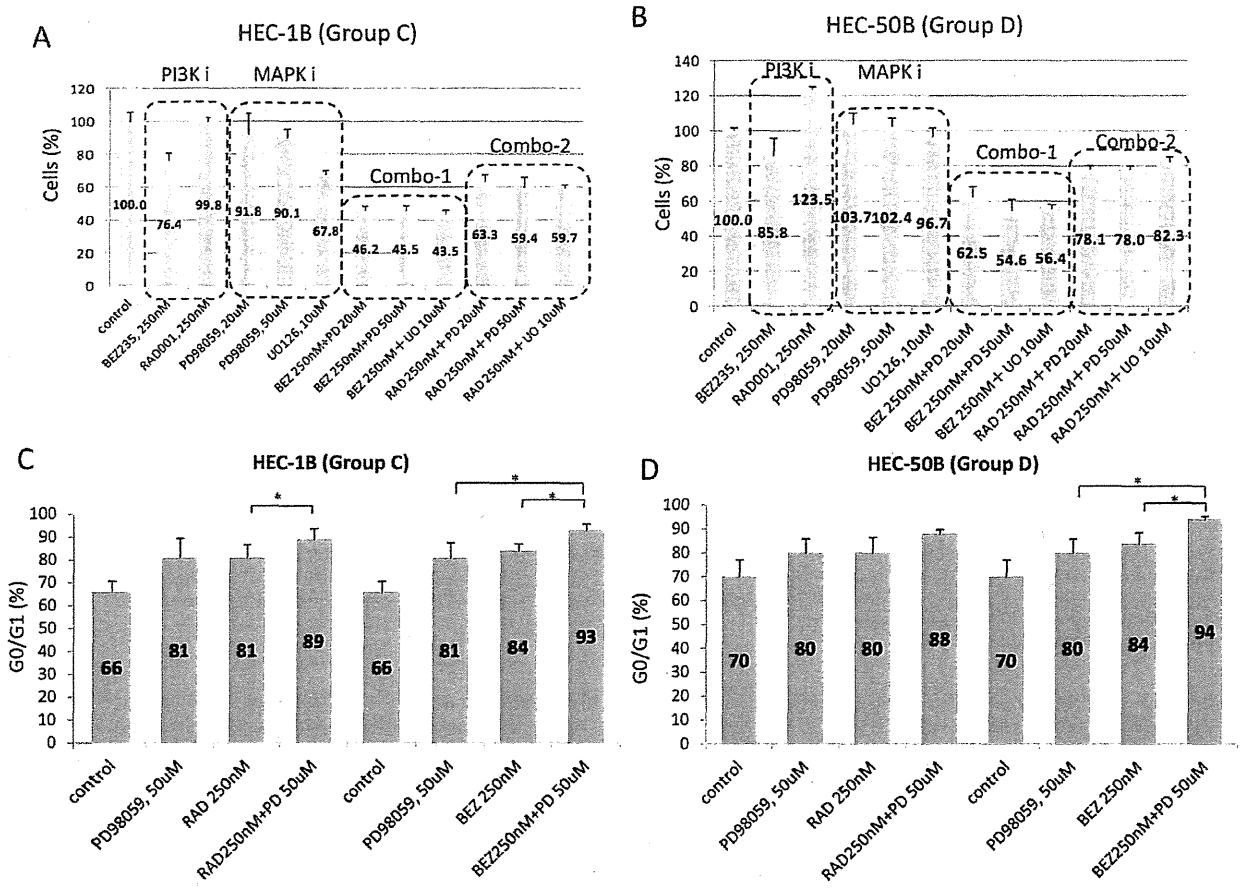

Figure 6. Inhibition of cell proliferation and augmentation of G1 arrest by combination of a MEK inhibitor and NVP-BEZ235 (or RAD001) in cells with alterations in *K-Ras* (mutation or amplification). (A)–(B) WST-8 assay was performed in HEC-1B (group C) and HEC-50B (group D) cell lines. All the experiments were repeated three times and each value is shown as the mean of three experiments +/− S.D. The combination of a MEK inhibitor (PD98059 or UO126) and NVP-BEZ235 (or RAD001) significantly augmented anti-proliferative effect in these cell lines, compared with either inhibition alone ($p<0.05$ by Student's t-test). (C)–(D) Flowcytometric analysis of cell cycle in HEC-1B and HEC-50B cells. All experiments were repeated 3 times, and each value is shown as the mean of 3 experiments ± S.D. Combination of a MEK inhibitor (PD98059 or UO126) and NVP-BEZ235 significantly augmented the percentage of cells in the G0-G1phase of the cell cycle in these cells. *: $p<0.05$ by Student's t-test.

doi:10.1371/journal.pone.0037431.g006

Developing predictive biomarkers in therapeutics targeting the PI3K/mTOR pathway is crucial, as alterations in several molecules are involved in the activation of this pathway. *PIK3CA* mutation and HER2 amplification have been recommended as useful biomarkers in breast cancer [26,35,36]. Mutant oncogenic Ras has been suggested as a dominant determinant of resistance in several solid tumor cells [19,37]. PTEN deficiency is controversial as a predictive biomarker [26,36,38]. The mechanism of resistance in PTEN-deficient tumors might be explained by the predominant activation of p110beta in *PTEN* mutant tumors [39,40], as NVP-BEZ235 and most of the other PI3K inhibitors suppress p110beta less preferentially than the other p110 isoforms. However, p110beta is not a predominant isoform in endometrial carcinomas with *PTEN* mutations [8]. The significance of p110alpha in *PTEN* mutant endometrial cancer would be helpful to identify patients susceptible to NVP-BEZ235. Thus, the existence of *PTEN* mutations might be a predictive biomarker for the PI3K/mTOR inhibitors in endometrial carcinomas. Further in vivo analysis, including the anti-tumor effect of NVP-BEA235, RAD001, or a combination of these compounds with a MEK inhibitor on groups C and D tumors would be necessary to evaluate the utility of these factors as biomarkers.

Feasibility of mutational analysis of the predictor genes should be also considered in clinical trials. *K-Ras* mutational analysis would be reasonably achievable, as "hot spot" mutations are located only in 2 exons (codons 12, 13, and 61). However, mutations of *PIK3CA* and *PTEN* are widespread in the entire coding region. Others and we have reported that PTEN expression is sufficiently evaluated by immunohistochemistry and is correlated with mutational status [25,41]. A combination of screening *K-Ras* mutations and immunohistochemistry analysis of PTEN might be a useful and feasible strategy in clinical trials of endometrial cancer. We previously reported that *PIK3CA* mutations frequently coexist with *K-Ras* muations in endometrial cancer [8]. The two group C cells (HEC-1B and HHUA) with double mutations of *PIK3CA* and *K-Ras* were less sensitive to NVP-BEZ235, compared with group A/B cells. Thus, *PIK3CA* mutation alone might not be a good biomarker in endometrial cancer. Over 5 clinical studies of the rapalogs have been developed in advanced endometrial cancer. Of them, Oza et al reported phase II study of

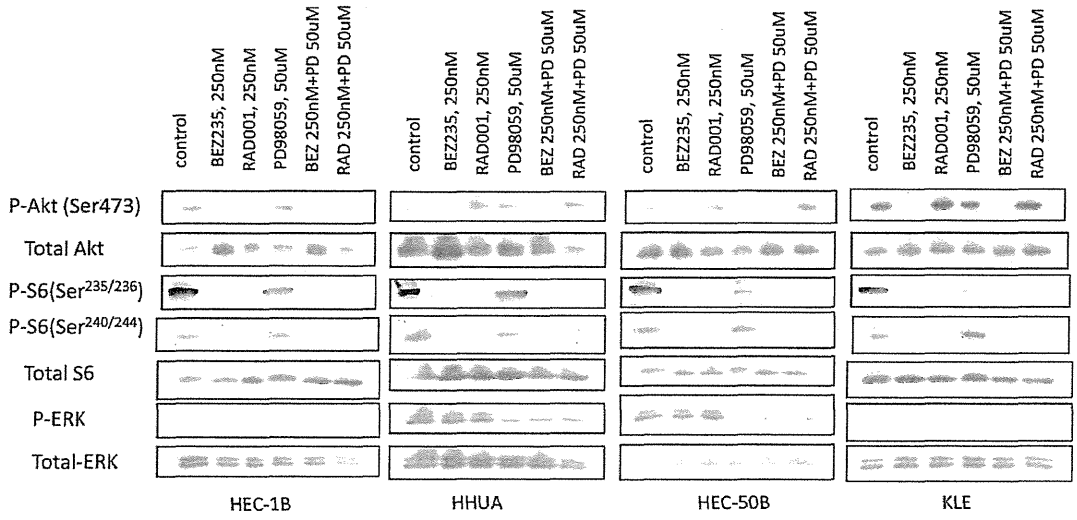

Figure 7. Inhibition of PI3K and MAPK signaling pathway by NVP-BEZ235, RAD001, and a MEK inhibitor (PD98059) in endometrial cancer cell lines with K-Ras alterations. Western blot analysis of total lysates of HEC-1B and HHUA (group C) and HEC-50B and KLE (group D) cells treated with 1 of the PI3K (or MAPK) signal inhibitors or their combination with 10% FBS. Phospho-Akt, phospho-S6, and phospho-ERK levels are shown with total Akt, total S6, and total ERK levels.
doi:10.1371/journal.pone.0037431.g007

temsirolimus in endometrial cancer, showing clinical benefit rate (partial response and stable disease) of 52% in chemoetherapy-treated patients [42]. They suggested that PTEN loss (immunohistochemistry and mutational analysis) and molecular markers of PI3K/Akt/mTOR pathway did not correlate with the clinical outcome. It would be clarified whether information of *K-Ras* alterations might be helpful in the clinical settings. As well, further exploration of the other PI3K-activating alterations (such as mutations of *FGFR2* and *PIK3R1*) and other measurable characteristics (such as standardized uptake value by PET imaging) would be also necessary to establish the most useful clinical biomarkers.

She et al reported that various cell lines with double mutations of *K-Ras/BRAF* and *PIK3CA* were resistant to AKT inhibitors, and suggested that a MEK inhibitor sensitizes these double mutant cells to AKT or PI3K inhibitors [43]. Our data in the two group C cells support that a combination of a MEK inhibitor and a PI3K (AKT) inhibitor might be effective to various types of cancers with double mutations of *K-Ras* and *PIK3CA*. In addition to mutations, copy number gain of oncogenes is also important for "oncogene addiction". We previously reported that extensive chromosomal instability (with 5 or more copy number alterations) is a poor independent prognostic factor in endometrial carcinomas [10]. Although extensive chromosomal instability is more common in type II endometrial carcinomas [44], the percentage of extensive chromosomal instability was 31% in our clinical endometrioid adenocarcinoma samples [10]. We found that both group D cell lines (KLE and HEC-50B) harbor extensive CNAs (copy number alterations), with copy number gain at the locus of *K-Ras*, although they do not possess any mutations in *K-Ras*, *PTEN* and *PIK3CA*. The antiproliferative effect of combined inhibition of MAPK pathway and PI3K/mTOR pathway in group D cells suggests that this combination therapy might be an option to treat tumors with CNA in *K-Ras*. The dual inhibition of the PI3K and MAPK pathways might overcome the resistance to PI3K/mTOR inhibition alone in certain endometrial tumors with *K-Ras* alterations through its enhanced cytostatic effect (at least in part). Cheung et al reported that endometrial cell lines with wild-type PI3K pathway members were resistant to an mTOR inhibitor, rapamycin, suggesting that other unexamined factors, including CNA in *K-Ras*, might be involved in the anti-tumor effect of rapalogs [45]. Phosphorylation of 4E-BP1 is not only regulated by mTORC1, but also by ERK signaling [43,46], suggesting the crosstalk between PI3K/mTOR pathway and MAPK pathway. It would be necessary to evaluate the in vivo effect of the combined therapy in tumors with *K-Ras* alterations to address the activity of the MAPK pathway in endometrial cancer.

Supporting Information

Figure S1 Inhibition of cell proliferation by NVP-BEZ235 in 13 endometrial cancer cells. The growth curves of all the 13 cells in response to NVP-BEZ235 in the WST-8 assay (in Figure 2) are shown in one graph.
(PPT)

Figure S2 Inhibition of cell proliferation by RAD001 in 13 endometrial cancer cells. The growth curves of all the 13 cells in response to RAD001 in the WST-8 assay (in Figure 2) are shown in one graph.
(PPT)

Figure S3 Flowcytometric analysis of cell cycle in cancer cells treated with either NVP-BEZ235 or RAD001. (A–D) Cells (5×10^5) were seeded and treated with NVP-BEZ235 or RAD001 for 48 h at a dose of 10 nM or 100 nM, respectively, as described in Figure 4. (A)–(B); The data from the two group C cells (HEC-1B and HHUA). (C)–(D); the data from the two group D cells (KLE and HEC-50B).
(PPT)

Figure S4 Inhibition of cell proliferation and augmentation of G1 arrest by combination of a MEK inhibitor and NVP-BEZ235 (or RAD001) in cells with alterations in *K-Ras* (mutation or amplification). (A)–(B) WST-8 assay was performed in HHUA (group C) and KLE (group D) cell lines. (C)–(D) Flowcytometric analysis of cell cycle in HHUA (group C) and

KLE (group D) cells. All experiments were repeated 3 times, and each value is shown as the mean of 3 experiments ± S.D.
(PPT)

Acknowledgments

We thank Masato Nishida for providing the Ishikawa3-H-12 cell line.

References

1. Yuan TL, Cantley LC (2008) PI3K pathway alterations in cancer: variations on a theme. Oncogene 27: 5497–5510.
2. Parkin DM (2001) Global cancer statistics in the year 2000. Lancet Oncol 2: 533–543.
3. Ryan AJ, Susil B, Jobling TW, Oehler MK (2005) Endometrial cancer. Cell Tissue Res 322: 53–61.
4. Doll A, Abal M, Rigau M, Monge M, Gonzalez M, et al. (2008) Novel molecular profiles of endometrial cancer-new light through old windows. J Steroid Biochem Mol Biol 108: 221–229.
5. Enomoto T, Inoue M, Perantoni AO, Buzard GS, Miki H, et al. (1991) K-ras activation in premalignant and malignant epithelial lesions of the human uterus. Cancer Res 51: 5308–5314.
6. Kong D, Suzuki A, Zou TT, Sakurada A, Kemp LW, et al. (1997) PTEN1 is frequently mutated in primary endometrial carcinomas. Nat Genet 17: 143–144.
7. Oda K, Stokoe D, Taketani Y, McCormick F (2005) High frequency of coexistent mutations of PIK3CA and PTEN genes in endometrial carcinoma. Cancer Res 65: 10669–10673.
8. Oda K, Okada J, Timmerman L, Rodriguez Viciana P, Stokoe D, et al. (2008) PIK3CA cooperates with other phosphatidylinositol 3′-kinase pathway mutations to effect oncogenic transformation. Cancer Res 68: 8127–8136.
9. Murayama Hosokawa S, Oda K, Nakagawa S, Ishikawa S, Yamamoto S, et al. (2010) Genome-wide single-nucleotide polymorphism arrays in endometrial carcinomas associate extensive chromosomal instability with poor prognosis and unveil frequent chromosomal imbalances involved in the PI3-kinase pathway. Oncogene 29: 1897–1908.
10. Hudes G, Carducci M, Tomczak P, Dutcher J, Figlin R, et al. (2007) Temsirolimus, interferon alfa, or both for advanced renal-cell carcinoma. N Engl J Med 356: 2271–2281.
11. Motzer RJ, Escudier B, Oudard S, Hutson TE, Porta C, et al. (2008) Efficacy of everolimus in advanced renal cell carcinoma: a double-blind, randomised, placebo-controlled phase III trial. Lancet 372: 449–456.
12. Motzer RJ, Escudier B, Oudard S, Hutson TE, Porta C, et al. (2010) Phase 3 trial of everolimus for metastatic renal cell carcinoma : final results and analysis of prognostic factors. Cancer 116: 4256–4265.
13. Houghton PJ (2010) Everolimus. Clin Cancer Res 16: 1368–1372.
14. Meric Bernstam F, Gonzalez Angulo AM (2009) Targeting the mTOR signaling network for cancer therapy. J Clin Oncol 27: 2278–2287.
15. Engelman JA (2009) Targeting PI3K signalling in cancer: opportunities, challenges and limitations. Nat Rev Cancer 9: 550–562.
16. Sarbassov DD, Guertin DA, Ali SM, Sabatini DM (2005) Phosphorylation and regulation of Akt/PKB by the rictor-mTOR complex. Science 307: 1098–1101.
17. Wullschleger S, Loewith R, Hall MN (2006) TOR signaling in growth and metabolism. Cell 124: 471–484.
18. Wan X, Harkavy B, Shen N, Grohar P, Helman LJ (2007) Rapamycin induces feedback activation of Akt signaling through an IGF-1R-dependent mechanism. Oncogene 26: 1932–1940.
19. Engelman JA, Chen L, Tan X, Crosby K, Guimaraes AR, et al. (2008) Effective use of PI3K and MEK inhibitors to treat mutant Kras G12D and PIK3CA H1047R murine lung cancers. Nat Med 14: 1351–1356.
20. Sos ML, Fischer S, Ullrich R, Peifer M, Heuckmann JM, et al. (2009) Identifying genotype-dependent efficacy of single and combined PI3K- and MAPK-pathway inhibition in cancer. Proc Natl Acad Sci U S A 106: 18351–18356.
21. Faber AC, Li D, Song Y, Liang MC, Yeap BY, et al. (2009) Differential induction of apoptosis in HER2 and EGFR addicted cancers following PI3K inhibition. Proc Natl Acad Sci U S A 106: 19503–19508.
22. Mordant P, Loriot Y, Leteur C, Calderaro J, Bourhis J, et al. (2010) Dependence on phosphoinositide 3-kinase and RAS-RAF pathways drive the activity of RAF265, a novel RAF/VEGFR2 inhibitor, and RAD001 (Everolimus) in combination. Mol Cancer Ther 9: 358–368.
23. Minaguchi T, Yoshikawa H, Oda K, Ishino T, Yasugi T, et al. (2001) PTEN mutation located only outside exons 5, 6, and 7 is an independent predictor of favorable survival in endometrial carcinomas. Clin Cancer Res 7: 2636–2642.
24. Samuels Y, Wang Z, Bardelli A, Silliman N, Ptak J, et al. (2004) High frequency of mutations of the PIK3CA gene in human cancers. Science 304: 554.
25. Shoji K, Oda K, Nakagawa S, Hosokawa S, Nagae G, et al. (2009) The oncogenic mutation in the pleckstrin homology domain of AKT1 in endometrial carcinomas. Br J Cancer 101: 145–148.
26. Serra V, Markman B, Scaltriti M, Eichhorn PJ, Valero V, et al. (2008) NVP-BEZ235, a dual PI3K/mTOR inhibitor, prevents PI3K signaling and inhibits the growth of cancer cells with activating PI3K mutations. Cancer Res 68: 8022–8030.
27. Cho DC, Cohen MB, Panka DJ, Collins M, Ghebremichael M, et al. (2010) The efficacy of the novel dual PI3-kinase/mTOR inhibitor NVP-BEZ235 compared with rapamycin in renal cell carcinoma. Clin Cancer Res 16: 3628–3638.
28. Liu TJ, Koul D, LaFortune T, Tiao N, Shen RJ, et al. (2009) NVP-BEZ235, a novel dual phosphatidylinositol 3-kinase/mammalian target of rapamycin inhibitor, elicits multifaceted antitumor activities in human gliomas. Mol Cancer Ther 8: 2204–2210.
29. McMillin DW, Ooi M, Delmore J, Negri J, Hayden P, et al. (2009) Antimyeloma activity of the orally bioavailable dual phosphatidylinositol 3-kinase/mammalian target of rapamycin inhibitor NVP-BEZ235. Cancer Res 69: 5835–5842.
30. Konstantinidou G, Bey EA, Rabellino A, Schuster K, Maira MS, et al. (2009) Dual phosphoinositide 3-kinase/mammalian target of rapamycin blockade is an effective radiosensitizing strategy for the treatment of non-small cell lung cancer harboring K-RAS mutations. Cancer Res 69: 7644–7652.
31. Brachmann SM, Hofmann I, Schnell C, Fritsch C, Wee S, et al. (2009) Specific apoptosis induction by the dual PI3K/mTor inhibitor NVP-BEZ235 in HER2 amplified and PIK3CA mutant breast cancer cells. Proc Natl Acad Sci U S A 106: 22299–22304.
32. Cao P, Maira SM, Garcia Echeverria C, Hedley DW (2009) Activity of a novel, dual PI3-kinase/mTor inhibitor NVP-BEZ235 against primary human pancreatic cancers grown as orthotopic xenografts. Br J Cancer 100: 1267–1276.
33. Maira SM, Stauffer F, Brueggen J, Furet P, Schnell C, et al. (2008) Identification and characterization of NVP-BEZ235, a new orally available dual phosphatidylinositol 3-kinase/mammalian target of rapamycin inhibitor with potent in vivo antitumor activity. Mol Cancer Ther 7: 1851–1863.
34. Mabuchi S, Altomare DA, Connolly DC, Klein Szanto A, Litwin S, et al. (2007) RAD001 (Everolimus) delays tumor onset and progression in a transgenic mouse model of ovarian cancer. Cancer Res 67: 2408–2413.
35. She QB, Chandarlapaty S, Ye Q, Lobo J, Haskell KM, et al. (2008) Breast tumor cells with PI3K mutation or HER2 amplification are selectively addicted to Akt signaling. PLoS One 3: e3065.
36. O'Brien C, Wallin JJ, Sampath D, GuhaThakurta D, Savage H, et al. (2010) Predictive biomarkers of sensitivity to the phosphatidylinositol 3′ kinase inhibitor GDC-0941 in breast cancer preclinical models. Clin Cancer Res 16: 3670–3683.
37. Ihle NT, Lemos R, Jr., Wipf P, Yacoub A, Mitchell C, et al. (2009) Mutations in the phosphatidylinositol-3-kinase pathway predict for antitumor activity of the inhibitor PX-866 whereas oncogenic Ras is a dominant predictor for resistance. Cancer Res 69: 143–150.
38. Dan S, Okamura M, Seki M, Yamazaki K, Sugita H, et al. (2010) Correlating phosphatidylinositol 3-kinase inhibitor efficacy with signaling pathway status: in silico and biological evaluations. Cancer Res 70: 4982–4994.
39. Jia S, Liu Z, Zhang S, Liu P, Zhang L, et al. (2008) Essential roles of PI(3)K-p110beta in cell growth, metabolism and tumorigenesis. Nature 454: 776–779.
40. Wee S, Wiederschain D, Maira SM, Loo A, Miller C, et al. (2008) PTEN-deficient cancers depend on PIK3CB. Proc Natl Acad Sci U S A 105: 13057–13062.
41. Yang J, Ren Y, Wang L, Li B, Chen Y, et al. (2010) PTEN mutation spectrum in breast cancers and breast hyperplasia. J Cancer Res Clin Oncol 136: 1303–1311.
42. Oza AM, Elit L, Tsao MS, Kamel Reid S, Biagi J, et al. (2011) Phase II study of temsirolimus in women with recurrent or metastatic endometrial cancer: a trial of the NCIC Clinical Trials Group. J Clin Oncol 29: 3278–3285.
43. She QB, Halilovic E, Ye Q, Zhen W, Shirasawa S, et al. (2010) 4E-BP1 is a key effector of the oncogenic activation of the AKT and ERK signaling pathways that integrates their function in tumors. Cancer Cell 18: 39–51.
44. Salvesen HB, Carter SL, Mannelqvist M, Dutt A, Getz G, et al. (2009) Integrated genomic profiling of endometrial carcinoma associates aggressive tumors with indicators of PI3 kinase activation. Proc Natl Acad Sci U S A 106: 4834–4839.
45. Cheung LW, Hennessy BT, Li J, Yu S, Myers AP, et al. (2011) High Frequency of PIK3R1 and PIK3R2 Mutations in Endometrial Cancer Elucidates a Novel Mechanism for Regulation of PTEN Protein Stability. Cancer Discov 1: 170–185.
46. Feldman ME, Apsel B, Uotila A, Loewith R, Knight ZA, et al. (2009) Active-site inhibitors of mTOR target rapamycin-resistant outputs of mTORC1 and mTORC2. PLoS Biol 7: e38.

Author Contributions

Conceived and designed the experiments: K. Shoji KO SN. Performed the experiments: K. Shoji T. Kashiyama YI Y. Miyamoto AM T. Koso. Analyzed the data: K. Shoji KO T. Kashiyama Y. Miyamoto HA. Contributed reagents/materials/analysis tools: SN K. Sone Y. Miyamoto HH MT Y. Matsumoto OW-H KK HK FM HA TY SK YT. Wrote the paper: K. Shoji KO.

Morita et al. Reproductive Biology and Endocrinology 2012, 10:14
http://www.rbej.com/content/10/1/14

REPRODUCTIVE BIOLOGY AND ENDOCRINOLOGY

RESEARCH Open Access

Resveratrol promotes expression of SIRT1 and StAR in rat ovarian granulosa cells: an implicative role of SIRT1 in the ovary

Yoshihiro Morita[1], Osamu Wada-Hiraike[1*], Tetsu Yano[1], Akira Shirane[1], Mana Hirano[1], Haruko Hiraike[1], Satoshi Koyama[1], Hajime Oishi[1], Osamu Yoshino[1], Yuichiro Miyamoto[1], Kenbun Sone[1], Katsutoshi Oda[1], Shunsuke Nakagawa[2], Kazuyoshi Tsutsui[3] and Yuji Taketani[1]

Abstract

Background: Resveratrol is a natural polyphenolic compound known for its beneficial effects on energy homeostasis, and it also has multiple properties, including anti-oxidant, anti-inflammatory, and anti-tumor activities. Recently, silent information regulator genes (Sirtuins) have been identified as targets of resveratrol. Sirtuin 1 (SIRT1), originally found as an NAD^+-dependent histone deacetylase, is a principal modulator of pathways downstream of calorie restriction, and the activation of SIRT1 ameliorates glucose homeostasis and insulin sensitivity. To date, the presence and physiological role of SIRT1 in the ovary are not known. Here we found that SIRT1 was localized in granulosa cells of the human ovary.

Methods: The physiological roles of resveratrol and SIRT1 in the ovary were analyzed. Immunohistochemistry was performed to localize the SIRT1 expression. SIRT1 protein expression of cultured cells and luteinized human granulosa cells was investigated by Western blot. Rat granulosa cells were obtained from diethylstilbestrol treated rats. The cells were treated with increasing doses of resveratrol, and subsequently harvested to determine mRNA levels and protein levels. Cell viability was tested by MTS assay. Cellular apoptosis was analyzed by caspase 3/7 activity test and Hoechst 33342 staining.

Results: SIRT1 protein was expressed in the human ovarian tissues and human luteinized granulosa cells. We demonstrated that resveratrol exhibited a potent concentration-dependent inhibition of rat granulosa cells viability. However, resveratrol-induced inhibition of rat granulosa cells viability is independent of apoptosis signal. Resveratrol increased mRNA levels of SIRT1, LH receptor, StAR, and P450 aromatase, while mRNA levels of FSH receptor remained unchanged. Western blot analysis was consistent with the results of quantitative real-time RT-PCR assay. In addition, progesterone secretion was induced by the treatment of resveratrol.

Conclusions: These results suggest a novel mechanism that resveratrol could enhance progesterone secretion and expression of luteinization-related genes in the ovary, and thus provide important implications to understand the mechanism of luteal phase deficiency.

Keywords: SIRT1, Resveratrol, Ovary, Granulosa cells, Luteinization

* Correspondence: osamu.hiraike@gmail.com
[1]Department of Obstetrics and Gynecology, Graduate School of Medicine, The University of Tokyo, 7-3-1, Hongo, Bunkyo-ku, Tokyo 113-8655, Japan
Full list of author information is available at the end of the article

Background

The study of natural compounds with pharmacological activity has become an emerging trend in nutritional and pharmacologic research. Polyphenols represent a vast group of compounds having aromatic ring, characterized by the presence of one or more hydroxyl groups with various structural complexities. Resveratrol (trans-3, 5, 40-trihydroxystilbene) is a natural polyphenol synthesized by plants as a phytoalexin that becomes activated under stress conditions such as ultraviolet radiation and fungal infection [1,2]. It can be found in berries, nuts and some medicinal plants, and mainly present in the skin of grapes and thus in red wine [3]. Previous studies have reported its anti-oxidant, anti-inflammatory, and growth-inhibitory activities using several cancer cell lines and animal models [2,4,5]. These properties of resveratrol have been linked to the inhibition of proliferation in association with cell cycle arrest and apoptotic cell death typically observed in vitro at concentrations in the range of 10-300 μM [5-7]. Thus, resveratrol has activity in regulating multiple cellular events associated with carcinogenesis, and the activation of SIRT1 is postulated to be a key event to elucidate the pathophysiology of resveratrol [8,9]. SIRT1, the mammalian homologue of yeast Sir2 (silent information regulator 2), functions as an NAD^+-dependent class III histone deacetylase. SIRT1 deacetylates multiple targets in mammalian cells, including p53, FOXO1, FOXO3, PGC-1α, liver X receptor, NBS1 and hypoxia-inducible factor 2α [10,11]. By regulating these molecules, SIRT1 functions as a master regulator of energy homeostasis, gene silencing, metabolism, genomic stability, and cell survival.

The ability of the ovary to produce growing follicles that ovulate is the basis of female fertilization. A critical feature of ovarian granulosa cell (GC) function is the differentiation of the ovulatory follicle into the corpus luteum which mainly produces progesterone (P4) that is important for the maintenance of pregnancy. Recently, it has been suggested that SIRT1 activator resveratrol plays a role in reproductive biology. Resveratrol was shown to modulate theca cell proliferation [12], and methylated resveratrol analogues possessed biological activities in swine GCs [13]. In the present study, to assess a role of SIRT1 in the regulation of reproductive axis in female, we investigated the expression of endogenous SIRT1 in human and rat GCs and the effect of resveratrol on cellular viability and steroidogenesis in rat GCs.

Methods

Chemicals

Diethylstilbestrol (DES) and resveratrol were purchased from Sigma-Aldrich (St. Louis, MO, USA). All other chemicals, unless otherwise mentioned, were obtained from Sigma-Aldrich.

Human cancer cell lines and primary human GCs

Human cervical cancer cell line HeLa was purchased from American Type Culture Collection (Manassas, VA, USA). Human ovarian granulosa-like tumor cell line KGN, which originated from a Stage III granulosa cell carcinoma in a 63-year-old Japanese women [14], was obtained from RIKEN Cell Bank of Japan (Tsukuba, Japan). Primary human GCs were obtained from patients undergoing transvaginal oocyte retrieval for in vitro fertilization at the University of Tokyo Hospital. The method to purify human GCs was described previously [15]. The study was approved by the Institutional Review Board of the University of Tokyo, and written informed consent for the research use of human GCs was obtained from each patient. These cells were maintained in Dulbecco's modified Eagle Medium (DMEM)/F12 medium (Invitrogen, Carlsbad, CA, USA) supplemented with 10% charcoal-stripped fetal bovine serum (FBS; Invitrogen), 100 U/ml penicillin, 100 μg/ml streptomycin and 0.25 μg/ml amphotericin B in a humidified atmosphere of 5% CO_2 and 95% air at 37°C.

Preparation and culture of rat GCs

Guidelines for the care and use of laboratory animals as adopted and promulgated by the University of Tokyo were followed. Twenty-three-day-old immature female Wistar rats were purchased from CLEA Japan, Inc. (Tokyo, Japan) and housed in a temperature-controlled room with a 12 h light/12 h dark schedule. Pelleted food and water were provided ad libitum. Rats were implanted with SILASTIC capsules (Dow Corning, Corp., Midland, MI, USA) containing 10 mg DES to increase GC number [16], and killed 4 days later by cervical dislocation. Removed ovaries were immediately cleaned of surrounding connective tissues and placed into DMEM/F12 medium supplemented with 10% charcoal-stripped FBS, 100 U/ml penicillin, 100 μg/ml streptomycin and 0.25 μg/ml amphotericin B. GCs were harvested by needle puncture of ovarian follicles, suspended in the medium, and purified by filtration with a 100-μm cell strainer and then a 40-μm cell strainer (BD Biosciences, Bedford, MA, USA). Isolated GCs were washed twice by centrifugation at 200 × g for 5 min and cultured in the medium in a humidified atmosphere of 5% CO_2 and 95% air at 37°C [17].

Tissue samples and immunohistochemistry

The ovarian tissues used in this study were obtained from 5 female patients with regular menstrual cycles who were taking no hormonal drugs and underwent

radical or extended hysterectomy for carcinoma of the uterine cervix and endometrium. The female patients were 32-44 years old at the time of operation and the operations were performed in proliferative phase of the menstrual cycle. The study was approved by the Institutional Review Board of the University of Tokyo, and written informed consent was obtained in each instance. Immunohistochemistry was performed as described previously [18]. Paraffin sections (4 μm) were dewaxed in xylene and rehydrated through graded ethanol to water. Antigens were retrieved by boiling in 10 mM citrate buffer (pH 6.0) for 30 min. The cooled sections were incubated in DAKO REAL Peroxidase-Blocking solution (DAKO, Carpinteria, CA, USA) for 30 min to quench endogenous peroxidase. To block the nonspecific binding, sections were incubated in PBS containing 3% BSA and 0.5% Nonidet P-40 for 10 min at room temperature. Sections were then incubated with the rabbit polyclonal antibody to SIRT1 (sc-15404, Santa Cruz Biotechnology, Inc., Santa Cruz, CA, USA) in DAKO REAL Antibody Diluent (DAKO) overnight at 4°C. Negative controls were incubated with preimmune serum IgG fraction. ChemMate EnVision Detection system (DAKO) was used to visualize the signal. The sections were developed with 3,3'-diaminobenzidine tetrahydrochloride substrate (DAKO), lightly counterstained with ae's hematoxylin (Wako Chemical, Tokyo, Japan), dehydrated through ethanol series and xylene, and mounted.

Western blotting

HeLa cells, KGN cells, and human GCs were seeded into 6-cm culture dishes (BD Biosciences) at a density of 1×10^6 cells/dish in 3 ml of the culture medium. After 48 h, the cells were harvested with trypsin (0.05%)/EDTA (0.02%) and scraped into the lysis buffer containing 50 mM Tris-HCl (pH 8.0), 150 mM NaCl, 0.02% sodium azide, 0.1% sodium dodecyl sulfate, 1% Nonidet P-40, and 0.5% sodium deoxycholate for 30 min on ice. Rat GCs were seeded into 10-cm culture dishes (BD Biosciences) at a density of $2\text{-}3 \times 10^6$ cells/dish in 10 ml of the culture medium. After 48 h, the medium was replaced with fresh medium containing 1% charcoal-stripped FBS and 100 μM of resveratrol, and cell culture was continued. Thereafter GCs were harvested, and lysed. Insoluble material was removed by centrifugation at 12,000 × g, for 20 min at 4°C. The supernatants were recovered, and the protein concentrations were measured using Bio-Rad protein assay reagent (Bio-Rad Lab., Hercules, CA, USA). Equivalent amounts of lysate protein (30 μg were subjected to 10% SDS-PAGE and electrophoretically transferred onto polyvinylidene difluoride membranes (Millipore Corp., Billerica, MA, USA). After blocking nonspecific binding sites by incubation for 1 h with Tris-buffered saline (25 mM Tris and 150 mM NaCl, pH 7.6) containing 5% nonfat milk and 0.2% Tween 20, the membranes were blotted with the primary antibodies overnight at 4°C. The primary antibodies used were anti-DBC1 [19] and anti-P450 aromatase (P450arom; MCA2077S, AbD serotec, Oxford, UK). Anti-SIRT1 (sc-15404), anti-StAR (sc-25806), and anti-LH receptor (LH-R; sc-25828) were purchased from Santa Cruz Biotechnology Inc. (Santa Cruz). Reactive proteins were detected with horseradish peroxidase-conjugated secondary antibodies (Cell Signaling Technology, Inc., Beverly, MA, USA) for 60 min at room temperature and developed with ECL Plus western blotting detection reagents (GE Healthcare, Little Chalfont, UK). The membranes were stripped with the buffer containing 100 mM 2-mercaptoethanol, 2% SDS and 62.5 mM Tris- HCl (pH 6.7), then reprobed with mouse monoclonal antibody to β-Actin (sc-47778, Santa Cruz Biotechnology, Inc.) to confirm equivalent protein loading. The images were scanned by the luminescent image analyzer Image Quant LAS 4000 mini (GE Healthcare).

Granulosa cell progesterone production

Culture media for the Western blot were collected, frozen, and stored at -20°C until P4 determination by Progesterone EIA kit (Cayman Chemical Co., Ann Arbor, MI, USA). P4 assay was performed according to the manufacture's instruction. The data are expressed as the amount of steroids (pg/ml) secreted. The results are representative of three to four independent cultures with each condition in quadruplet.

Cell viability assay

Viability of rat GCs was examined by using the 3-(4,5-dimethylthiazol-2-yl)-5- (3-carboxymethoxyphenyl)-2-(4-sulfophenyl)-2H-tetrazolium, inner salt (MTS) assay kit (CellTiter 96 Aqueous One Solution Cell Proliferation Assay; Promega, Madison, WI, USA) according to the manufacturer's instructions. Briefly, cells were seeded into 96-well plates (BD Biosciences) at a density of 1×10^4 cells/well in 100 μL of the culture medium. After 48 h, the medium was replaced with fresh medium containing 1% charcoal-stripped FBS and various concentrations of resveratrol, and cell culture was continued for a further 72 h. Resveratrol was dissolved in dimethyl sulfoxide and diluted with the medium to yield desired concentrations. The final concentration of dimethyl sulfoxide never exceeded 0.05%. The effects of resveratrol were investigated at concentrations between 10 and 100 μM in consideration of those used in the other studies where resveratrol inhibited the proliferation of various cell types at concentrations in the range of 10-300 μM [5-7]. Finally, the medium was replaced with 100 μL of fresh medium containing 20 μL of MTS solution and incubated for an additional 4 h. Mitochondrial

dehydrogenase enzymes of viable cells converted MTS tetrazolium into a colored formazan product. The optical density of samples was read at 490 nm in the spectrophotometric microplate reader (BioTek, Winooski, VT, USA).

Reverse transcription and quantitative real-time PCR

Rat GCs were seeded into 6-cm culture dishes (BD Biosciences) at a density of 1×10^6 cells/dish in 3 ml of the culture medium. After 48 h, the medium was replaced with fresh medium containing 1% charcoal-stripped FBS and various concentrations of resveratrol (10-100 μM, and cell culture was continued for a further 24 h. Total cellular RNA was extracted using RNeasy Mini Kit (Qiagen, Hilden, Germany) and quantified by measuring absorbance at 260 nm and stored at -80° until assay. The mRNA levels of relevant molecules were measured by quantitative real-time RT-PCR using One Step SYBR PrimeScript RT-PCR Kit (TaKaRa Bio. Inc., Tokyo, Japan) in the Light Cycler (Roche Applied Science, Mannheim, Germany). Accumulated levels of fluorescence were analyzed by the second-derivative method after the melting-curve analysis, and then the expression levels of target genes were normalized to the expression level of β-Actin in each sample. Primer pairs of analyzed mRNA are described in Table 1.

Table 1 Primer sequences used for quantitative real-time PCR

Gene	Primers	Primer Sequence	Expected size in base pair
β-actin	Sense	CGAGTACAACCTTCTTGCAG	207
	Antisense	TTCTGACCCATACCCACCAT	
Bax	Sense	GAATTGGCGATGAACTGGAC	157
	Antisense	GCAAAGTAGAAAAGGGCAACC	
Bcl2	Sense	AACATCGCTCTGTGGATGAC	150
	Antisense	GAGCAGCGTCTTCAGAGACA	
DBC1	Sense	TCTCCAAGTCTCGCCTGTG	158
	Antisense	CTCTGTTGCCTCCAACCAGT	
FSH-R	Sense	ATGGCCCCCATTTCATTCTT	82
	Antisense	ACTAGGAGAATCTTGGCCTTGGA	
LH-R	Sense	ATTGACACTCTGCTTAACTTTCCATCT	82
	Antisense	TGGCCATGAGGTACTCATGATCT	
p450arom	Sense	TCCTCAGCAGAGAAACTGGAAGA	151
	Antisense	CGTACAGAGTGACGGACATGGT	
SIRT1	Sense	TGTTTCCTGTGGGATACCTGA	137
	Antisense	TGAAGAATGGTCTTGGGTCTTT	
StAR	Sense	AGGAAAACAGAACTGAGGCTTAGAATA	93
	Antisense	AAGGTTTCATAGATACCTGTCCCTTAAC	

Caspase-3/7 activity assay

Apoptosis executioner caspase-3/7 activity in rat GCs was measured using the Apo-ONE Homogeneous Caspase-3/7 Assay kit (Promega) according to the manufacturer's instructions. Briefly, cells were seeded into 96-well plates (BD Biosciences) at a density of 1×10^4 cells/well in 100 μL of the culture medium. After 48 h, the medium was replaced with fresh medium containing 1% charcoal-stripped FBS and various concentrations of resveratrol (10- 100 μM), and cell culture was continued for 6, 12 and 24 h. Caspase-3/7 activity was measured at excitation wavelength 485 nm and emission wavelength 528 nm in the spectrophotometric microplate reader (BioTek).

Hoechst 33342 nuclear staining

Hoechst staining was performed to confirm the apoptotic profile as a result of morphological change in the nucleus in which Hoechst 33342 binds specifically to A-T base region in DNA and emits fluorescence. Rat GCs were seeded into 8-well chamber slides (Nalge Nunc International, Naperville, IL, USA) at a density of 1×10^5 cells/well in 400 μl of the culture medium. After 48 h, the medium was replaced with fresh medium containing 1% charcoal-stripped FBS and resveratrol (50 and 100 μM), and cell culture was continued for 6, 12, 24 and 48 h. Finally, cells were rinsed in PBS and fixed with 4% paraformaldehyde in PBS (pH 7.4) at room temperature for 30 min. Then cells were rinsed in PBS twice and stained with Hoechst 33342 (10 μg/ml in PBS) for 3 min. The specimens were mounted with Vectashield medium (Vector Labs. Inc., Burlingame, CA, USA) and photographs were taken at X200 magnification under a fluorescent confocal microscope (Carl-Zeiss MicroImaging Inc., Oberkochen, Germany).

Statistical analysis

Data represent the mean ± SEM from at least three independent experiments. Statistical analyses were carried out by one-way ANOVA with *post-hoc* test for multiple comparisons by using StatView software (SAS Institute Inc., Cary, NC, USA). $P < 0.05$ was considered statistically significant.

Results

Expression of SIRT1 protein in human GCs

We investigated the localization of SIRT1 protein in the human ovary using immunohistochemistry. Expression of SIRT1 was observed in nuclei of GCs at various stages of follicular development (Figure 1A-C). Part of the theca interstitial cells and the oocyte were also found to have positive signals. To confirm the expression of SIRT1, luteinized human granulosa cells were obtained from women undergoing in vitro fertilization

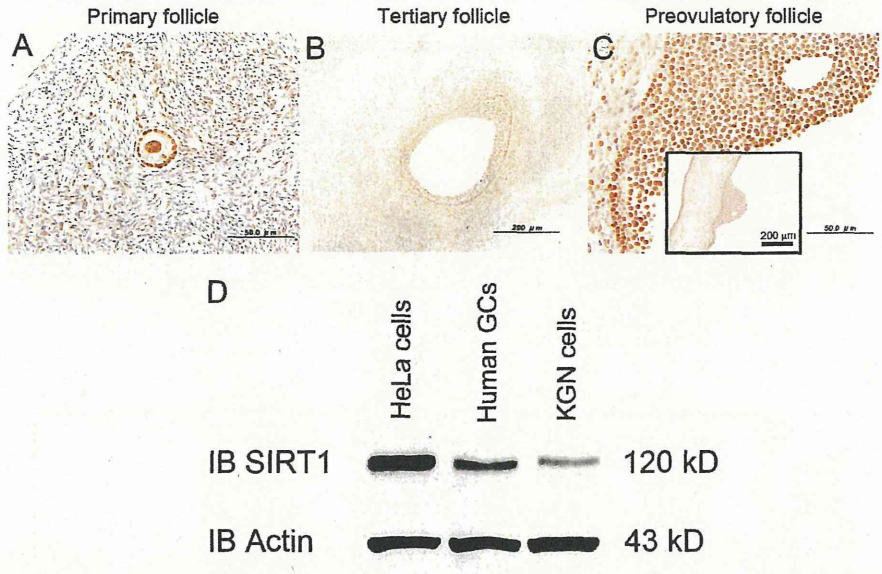

Figure 1 Expression of SIRT1 protein in human GCs. Immunohistochemical detection of SIRT1 in the human ovary (A, primary follicle; B, tertiary follicle; C, preovulatory follicle). Representative data from five specimens were shown. Nuclei of GCs were positively stained with anti-SIRT1 antibody at various stages of follicular development. Bars indicate (A) 50 μm, (B) 200 μm, and (C) 50 μm in high-power field and 200 μm in low-power field. SIRT1 was detected in primary (A), tertiary (B), and preovulatory (C) follicles of granulosa cells. Note that a part of the theca cells and oocyte nucleus are stained. Negative controls included a section incubated with preimmune rabbit IgG. (D) Western blotting revealed the presence of SIRT1 in KGN cells, human GCs, and HeLa cells (positive control).

program, and Western blot analysis revealed the expression of SIRT1 protein in KGN cells and human GCs (Figure 1D). HeLa cells were used as a positive control for Western blot because we [19] and other investigators [20] have detected the expression of SIRT1 protein.

Effect of resveratrol on cell viability and expression of SIRT1 and DBC1 in cultured rat GCs

To determine whether activation of SIRT1 by resveratrol affects rat GC viability, the extent of cell viability was measured by MTS assay. Resveratrol, at concentrations between 50 and 100 μM, produced a dose-dependent inhibition of cell viability after 72 h of treatment, with the maximal effect (reduction to 22.8 ± 4.4% of the control) being observed at 100 μM (Figure 2A). Recent studies have shown that DBC1 promotes p53-mediated apoptosis through specific inhibition of deacetylase activity of SIRT1 [21,22]. To determine whether the inhibitory effect on cell viability by resveratrol is related to the change in SIRT1 activation, the effect of resveratrol on mRNA levels of SIRT1 and DBC1, a negative regulator of SIRT1, was investigated by quantitative real-time RT-PCR in cultured rat GCs. After 24 h culture of rat GCs, mRNA levels of SIRT1 significantly increased at 100 μM (Figure 2B), while those of DBC1 remained unchanged (Figure 2C). Western blot analysis was also performed to confirm the result of quantitative real time RT-PCR and resveratrol-dependent induction of SIRT1 protein was observed (Figure 2D)

Effect of resveratrol on cell-death machinery in cultured rat GCs

Resveratrol has been shown to induce cell-cycle arrest and apoptosis in various cell lines [5,12]. To determine whether the reduction of the viability of rat GCs by resveratrol is due to the induction of apoptosis, the effect of resveratrol on mRNA levels of the representative apoptosis promoter Bax and inhibitor Bcl-2 was analyzed by quantitative real-time RT-PCR in cultured rat GCs at concentrations of resveratrol between 10 and 100 μM. The significant change in mRNA levels of Bax and Bcl-2 was not found at 24 h (Figure 3A, B). Apoptosis executioner caspase-3/7 activity was measured in cultured rat GCs at concentrations of resveratrol ranging from 10 to 100 μM and at various time points (6, 12, and 24 h). Resveratrol significantly inhibited caspase-3/7 activity at 75 and 100 μM after 24 h of treatment (Figure 3C). Furthermore, the effect of resveratrol on the incidence of apoptotic cells was investigated by Hoechst 33342 nuclear staining. Resveratrol (50 and 100 μM) showed no typical apoptotic changes including nuclear shrinkage, chromatin condensation, and nuclear fragmentation in cultured rat GCs at 6, 12, 24, and 48 h (Figure 3D).

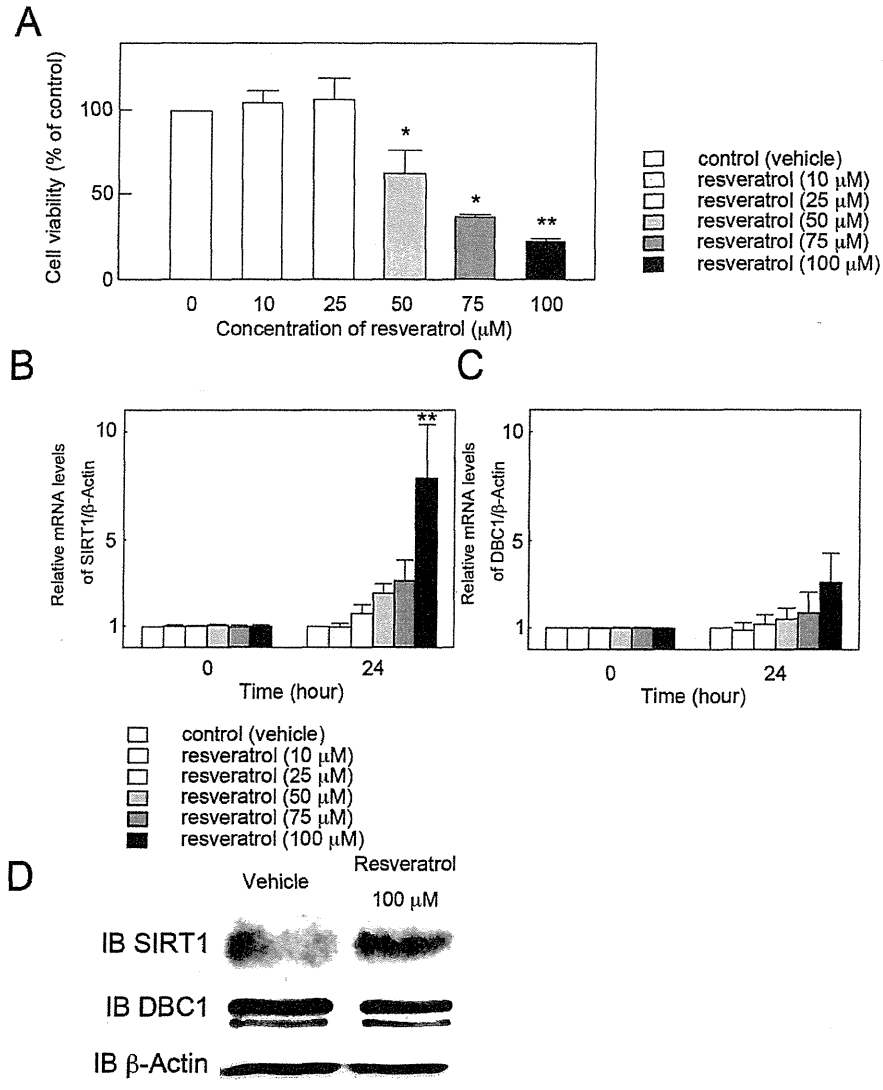

Figure 2 Effect of resveratrol on cell viability and expression of SIRT1 and DBC1 in cultured rat GCs. (A) Effect of resveratrol on cell viability at 72 h was estimated by MTS assay. Results are shown as the mean percentage of the untreated control ± SEM (bars) of eight wells of three independent experiments * $p < 0.05$ *vs.* control. ** $p < 0.01$ *vs.* control. (B and C) Effect of resveratrol on mRNA levels of (B) SIRT1 and (C) DBC1 was investigated by quantitative real-time RT-PCR. The mRNA level of the untreated control was arbitrarily set at 1.0, and that of the treatment group was estimated relative to the control value. Results are shown as the mean ± SEM (bars) of three independent experiments. ** $p < 0.01$ *vs.* control. (D) Effect of resveratrol on protein levels of SIRT1 was investigated by Western blot. Resveratrol treatment resulted in an increased expression of SIRT1 protein, and the results were consistent with that of quantitative real time RT-PCR. Three independent experiments were performed and a representative result is shown.

Effect of resveratrol on folliculogenesis-related molecules in cultured rat GCs

The Effect of resveratrol on mRNA levels of folliculogenesis-related molecules was investigated by quantitative real-time RT-PCR in cultured rat GCs at concentrations of resveratrol between 10 and 100 μM. After 24 h culture, resveratrol significantly increased mRNA levels of LH-R, steroidogenic acute regulatory protein (StAR), and P450arom at 100 μM (Figure 4B-D), while FSH receptor (FSH-R) mRNA levels remained unchanged (Figure 4A). Western blot analysis was also performed to confirm the result of quantitative real time RT-PCR and resveratrol-dependent stimulation of StAR, LH-R, and P450arom protein was confirmed (Figure 4E). To investigate the possibility that resveratrol promote steroidgenesis, serum concentration of P4 was evaluated and it has been revealed that resveratrol exhibited 3-fold enhancement of hormonal secretion at 48 h of culture (Figure 4F).

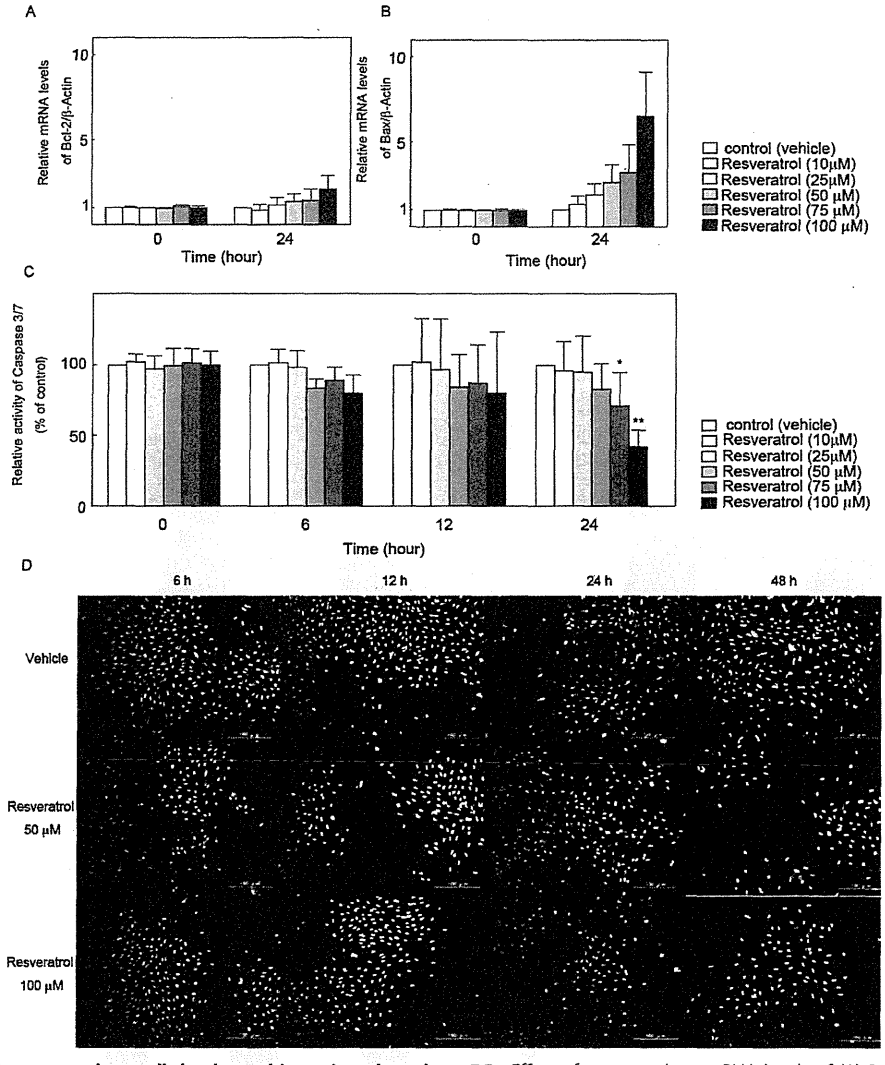

Figure 3 Effect of resveratrol on cell-death machinery in cultured rat GCs. Effect of resveratrol on mRNA levels of (A) Bcl-2 and (B) Bax was investigated by quantitative real-time RT-PCR. The mRNA level of the untreated control was arbitrarily set at 1.0, and that of the treatment group was estimated relative to the control value. Results are shown as the mean ± SEM (bars) of three independent experiments. (C) Caspase-3/7 activity was measured by the Apo-ONE Homogeneous Caspase-3/7 Assay kit at 6, 12 and 24 h. Results are shown as the mean percentage of the untreated control ± SEM (bars) of eight wells of three independent experiments. (D) Hoechst 33342 staining of resveratrol-treated rat GCs at 6, 12, 24, and 48 h. * $p < 0.05$ *vs.* control. ** $p < 0.01$ *vs.* control.

Discussion

Recently, resveratrol has been the focus of many *in vitro* and *in vivo* studies because of its pleiotropic biological activities [1-9]. However, the studies of resveratrol in ovarian physiology are limited. Resveratrol has been reported to exert estrogenic effects, increasing uterine and ovarian wet weight [23]. It is a phytoestrogen known to bind equally to estrogen receptors α and β [24], and structurally similar to synthetic estrogens, such as DES and 17β-estradiol benzoate [25]. In contrast to its hyperproliferative effects, resveratrol promoted apoptosis in rat ovarian theca-interstitial cells [12], and its analogues inhibited swine GC growth [13]. It was also reported that resveratrol inhibited the proliferation of a wide variety of human cancer cell lines through the induction of S-phase cell cycle arrest and apoptosis [5]. In the present study, we demonstrated that resveratrol exerted a dose-dependent inhibition of cell viability on rat GCs. This effect appeared not to be due to the induction of apoptosis, which was different from the previous findings in rat ovarian theca-interstitial cells [12]. Then we studied whether this resveratrol-induced decrease of cellular viability may lead to the differentiation of GCs.

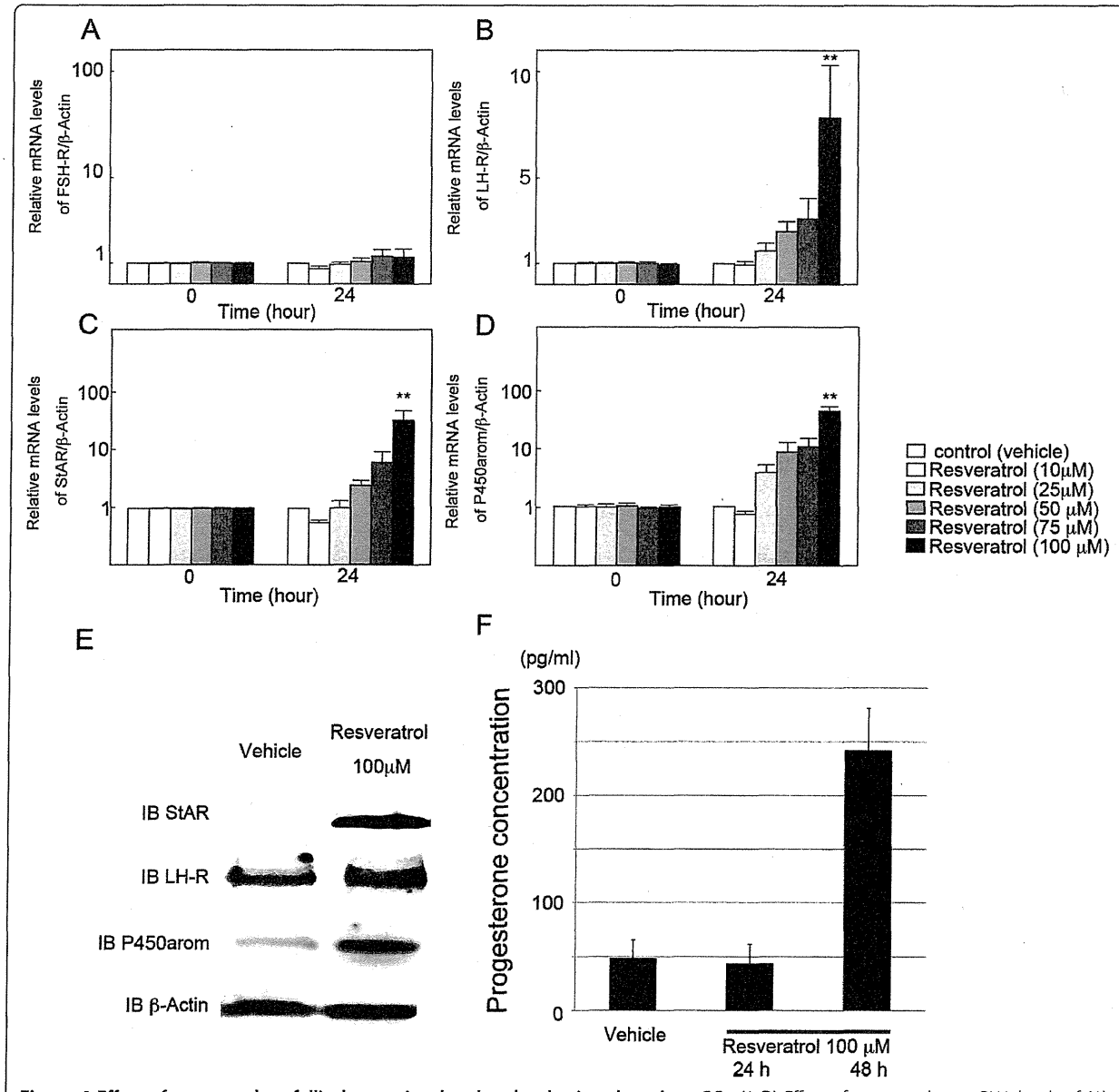

Figure 4 Effect of resveratrol on folliculogenesis-related molecules in cultured rat GCs. (A-D) Effect of resveratrol on mRNA levels of (A) FSH-R, (B) LH-R, (C) StAR and (D) P450arom was investigated by quantitative real-time RT-PCR. The mRNA level of the untreated control was arbitrarily set at 1.0, and that of the treatment group was estimated relative to the control value. Results are shown as the mean ± SEM (bars) of three independent experiments. ** $p < 0.01$ *vs.* control. (E) Effect of resveratrol on protein levels of StAR and P450arom was investigated by Western blot. Resveratrol treatment resulted in an increased expression of StAR, LH-R, and P450arom, and the results were consistent with those of quantitative real time RT-PCR. Three independent experiments were performed and a representative result is shown. (F) Effect of resveratrol on P4 secretion by rat granulosa cells. P4 secretion was measured by EIA protocol in culture medium of granulosa cells after 24 to 48 h of culture in DMEM/F-11 medium in the presence of resveratrol (100 μM). The data are expressed as the amount of steroids (pg/ml) secreted. The results, expressed as means ± SEM, are representative of three to four independent cultures with each condition in quadruplet.

Sirtuins are a conserved family of NAD^+-dependent class III histone deacetylases involved in a number of cellular processes including gene silencing at telomere and mating loci, DNA repair, recombination, and aging [8,10,11]. Recent studies have established that SIRT1 plays an important role in the regulation of cell fate and stress response in mammalian cells, and promotes cell survival by inhibiting apoptosis or cellular senescence induced by stresses including DNA damage [11]. Indeed, resveratrol administration and accompanying activation

of SIRT1 has improved health and survival of mice on a high-calorie diet by ameliorating insulin resistance [9]. Here we demonstrated the expression of SIRT1 in human GCs by immunohistochemical and Western blot analysis, and the expression of its mRNA in rat GCs by RT-PCR. To our knowledge, this is the first report that SIRT1 is expressed in the ovarian follicular cells. It is also interesting that resveratrol treatment caused an increase in SIRT1 mRNA levels as well as the stimulation of the deacetylating function of SIRT1. Similar to this result, the mouse experimental model of dextran sodium sulfate-induced colitis was associated with a decrease in SIRT1 gene expression and resveratrol treatment significantly reversed the expression of SIRT1 [26]. However, it should be noted that all actions of resveratrol are not related to the activation of SIRT1 because resveratrol is an indirect activator of SIRT1 and has been shown to activate the expression and activity of nicotinamide phosphoribosyltransferase and AMP-activated protein kinase (AMPK) [27-30].

In our study, resveratrol increased the expression of P450arom and luteinization-related molecules, such as LH-R and StAR, in rat GCs, suggesting a possibility that resveratrol may promote steroidogenesis and luteinization, a process of terminal differentiation of GCs, in the ovary. In fact, P4 secretion was increased after resveratrol treatment. These findings are consistent with the previous study using HL60 promyelocytic cell line [31]. Since mRNA levels of LH-R in the human corpus luteum were reported to be about 7 times higher than those in preovulatory follicles [32], LH-R has been thought to be a key factor in the ability of GC to undergo luteinization. In the human and other primates, StAR is also essential for the development and maintenance of the corpus luteum. StAR is known to govern the rate-limiting step in steroidogenesis, which is the translocation of cholesterol from the outer to the inner mitochondrial membrane [33]. The process of luteinization is associated with up-regulation of StAR in luteinized granulosa cells. Considering the fact that StAR is not highly expressed in GCs of preovulatory follicles [34], our data may implicate a role of SIRT1 and its activator in promoting luteinization of the ovary. Following ovulation, GCs undergo luteinization and form the corpus luteum which secretes P4. Secretion of P4 is indispensable to cause secretory transformation of the endometrium so that implantation can occur. Before the placenta takes over P4 production, P4 produced by the corpus luteum provides the necessary support to early pregnancy. A defect in the corpus luteum function is associated with implantation failure and miscarriage [35]. Here we showed a new insight that the resveratrol treatment may serve, at least in part, as luteal support. Physiological roles of resveratrol in the ovary should be further determined because another possible beneficial effect on ovarian physiology is reported. Resveratrol is known as a pure aryl hydrocarbon receptor antagonist with no agonistic activity. Polycyclic aromatic hydrocarbons are environmental toxicants found in cigarette smoke, and stimulate aryl hydrocarbon receptor. Polycyclic aromatic hydrocarbons have detrimental effect on ovarian reserve via inducing Harakiri, and resveratrol may exert its rescuing effect by inhibiting Harakiri expression [36]. However, in view of the significant difference in the ovarian physiology between humans and rodents, our data should be interpreted with caution and the present observations should be verified using human GCs.

Conclusions

We have demonstrated that resveratrol plays a key role in the activation of luteinization, the terminal differentiation of GCs, and exerts its effects by stimulating the expression of SIRT1, StAR, LH-R, and P450arom in GCs. As a result of these effects, we found that resveratrol promoted P4 secretion. These results suggest that the stimulation of SIRT1 by resveratrol would be potentially beneficial in the treatment of luteal phase deficiency. Several chemical compounds are known to affect the SIRT1 activities, and SIRT1 stimulators are currently extensively investigated for the treatment of diabetes. We hypothesize that these drugs might have a role in ovarian physiology by affecting SIRT1, but further studies are necessary to confirm the physiological implication of SIRT1 in the ovary.

Abbreviations

DES: Diethylstilbestrol; DMEM: Dulbecco's Modified Eagle Medium; FBS: Fetal bovine serum; FSH-R: Follicle stimulating hormone receptor; GC: Granulosa cell; LH-R: Luteinizing hormone receptor; P4: Progesterone; P450arom: P450 aromatase; RT-PCR: Reverse transcript-polymerase chain reaction; StAR: Steroidogenic acute regulatory protein.

Acknowledgements

This study was supported by Grant-in-Aid for Scientific Research from the Ministry of Education, Science and Culture, JMS Bayer Schering Pharma Grant, Kowa Life Science Foundation, and Kanzawa Medical Research Foundation, Japan.

Author details

[1]Department of Obstetrics and Gynecology, Graduate School of Medicine, The University of Tokyo, 7-3-1, Hongo, Bunkyo-ku, Tokyo 113-8655, Japan. [2]Department of Obstetrics and Gynecology, School of Medicine, Teikyo University, 2-11-1 Kaga, Itabashi-ku, Tokyo 173-8605, Japan. [3]Laboratory of Integrative Brain Sciences, Department of Biology, Waseda University, 2-2, Wakamatsuchou, Shinjuku-ku, Tokyo, 162-8480, Japan.

Authors' contributions

YM carried out all of the experiments. AS, MH, HH, YM, and KS participated in the immunohistochemistry, real time PCR, Western blot, and hormonal quantification. OY helped to collect and purify rat GCs. SK, MH, and HO helped to collect human luteinized GCs from follicular aspirates. OW-H has been involved in acquisition of data, drafting the manuscript, and revising it critically for important intellectual content. KO, SN, and TY have made

substantial contributions to conception and design, analysis and interpretation of data. KT and YT have given final approval of the version to be submitted. All authors read and approved the final manuscript.

Competing interests
The authors declare that they have no competing interests.

Received: 5 September 2011 Accepted: 23 February 2012
Published: 23 February 2012

References

1. Langcake P, Pryce RJ: **A new class of phytoalexins from grapevines.** *Experientia* 1977, **33(2)**:151-152.
2. Gusman J, Malonne H, Atassi G: **A reappraisal of the potential chemopreventive and chemotherapeutic properties of resveratrol.** *Carcinogenesis* 2001, **22(8)**:1111-1117.
3. Jang M, Cai L, Udeani GO, Slowing KV, Thomas CF, Beecher CW, Fong HH, Farnsworth NR, Kinghorn AD, Mehta RG, *et al*: **Cancer chemopreventive activity of resveratrol, a natural product derived from grapes.** *Science* 1997, **275(5297)**:218-220.
4. Manna SK, Mukhopadhyay A, Aggarwal BB: **Resveratrol suppresses TNF-induced activation of nuclear transcription factors NF-kappa B, activator protein-1, and apoptosis: potential role of reactive oxygen intermediates and lipid peroxidation.** *J Immunol* 2000, **164(12)**:6509-6519.
5. Joe AK, Liu H, Suzui M, Vural ME, Xiao D, Weinstein IB: **Resveratrol induces growth inhibition, S-phase arrest, apoptosis, and changes in biomarker expression in several human cancer cell lines.** *Clin Cancer Res* 2002, **8(3)**:893-903.
6. van Ginkel PR, Sareen D, Subramanian L, Walker Q, Darjatmoko SR, Lindstrom MJ, Kulkarni A, Albert DM, Polans AS: **Resveratrol inhibits tumor growth of human neuroblastoma and mediates apoptosis by directly targeting mitochondria.** *Clin Cancer Res* 2007, **13(17)**:5162-5169.
7. Issuree PD, Pushparaj PN, Pervaiz S, Melendez AJ: **Resveratrol attenuates C5a-induced inflammatory responses in vitro and in vivo by inhibiting phospholipase D and sphingosine kinase activities.** *FASEB J* 2009, **23(8)**:2412-2424.
8. Howitz KT, Bitterman KJ, Cohen HY, Lamming DW, Lavu S, Wood JG, Zipkin RE, Chung P, Kisielewski A, Zhang LL, *et al*: **Small molecule activators of sirtuins extend Saccharomyces cerevisiae lifespan.** *Nature* 2003, **425(6954)**:191-196.
9. Baur JA, Pearson KJ, Price NL, Jamieson HA, Lerin C, Kalra A, Prabhu VV, Allard JS, Lopez-Lluch G, Lewis K, *et al*: **Resveratrol improves health and survival of mice on a high-calorie diet.** *Nature* 2006, **444(7117)**:337-342.
10. Michan S, Sinclair D: **Sirtuins in mammals: insights into their biological function.** *Biochem J* 2007, **404(1)**:1-13.
11. Finkel T, Deng CX, Mostoslavsky R: **Recent progress in the biology and physiology of sirtuins.** *Nature* 2009, **460(7255)**:587-591.
12. Wong DH, Villanueva JA, Cress AB, Duleba AJ: **Effects of resveratrol on proliferation and apoptosis in rat ovarian theca-interstitial cells.** *Mol Hum Reprod* 2010, **16(4)**:251-259.
13. Basini G, Tringali C, Baioni L, Bussolati S, Spatafora C, Grasselli F: **Biological effects on granulosa cells of hydroxylated and methylated resveratrol analogues.** *Mol Nutr Food Res* 2010, **54(Suppl 2)**:S236-243.
14. Nishi Y, Yanase T, Mu Y, Oba K, Ichino I, Saito M, Nomura M, Mukasa C, Okabe T, Goto K, *et al*: **Establishment and characterization of a steroidogenic human granulosa-like tumor cell line, KGN, that expresses functional follicle-stimulating hormone receptor.** *Endocrinology* 2001, **142(1)**:437-445.
15. Shi J, Yoshino O, Osuga Y, Nishii O, Yano T, Taketani Y: **Bone morphogenetic protein 7 (BMP-7) increases the expression of follicle-stimulating hormone (FSH) receptor in human granulosa cells.** *Fertil Steril* 2010, **93(4)**:1273-1279.
16. Otsuka F, Moore RK, Wang X, Sharma S, Miyoshi T, Shimasaki S: **Essential role of the oocyte in estrogen amplification of follicle-stimulating hormone signaling in granulosa cells.** *Endocrinology* 2005, **146(8)**:3362-3367.
17. Chen Q, Yano T, Matsumi H, Osuga Y, Yano N, Xu J, Wada O, Koga K, Fujiwara T, Kugu K, *et al*: **Cross-Talk between Fas/Fas ligand system and nitric oxide in the pathway subserving granulosa cell apoptosis: a possible regulatory mechanism for ovarian follicle atresia.** *Endocrinology* 2005, **146(2)**:808-815.
18. Wada-Hiraike O, Hiraike H, Okinaga H, Imamov O, Barros RP, Morani A, Omoto Y, Warner M, Gustafsson JA: **Role of estrogen receptor beta in uterine stroma and epithelium: Insights from estrogen receptor beta-/- mice.** *Proc Natl Acad Sci USA* 2006, **103(48)**:18350-18355.
19. Hiraike H, Wada-Hiraike O, Nakagawa S, Koyama S, Miyamoto Y, Sone K, Tanikawa M, Tsuruga T, Nagasaka K, Matsumoto Y, *et al*: **Identification of DBC1 as a transcriptional repressor for BRCA1.** *Br J Cancer* 2010, **102(6)**:1061-1067.
20. Kim JE, Lou Z, Chen J: **Interactions between DBC1 and SIRT 1 are deregulated in breast cancer cells.** *Cell Cycle* 2009, **8(22)**:3784-3785.
21. Kim JE, Chen J, Lou Z: **DBC1 is a negative regulator of SIRT1.** *Nature* 2008, **451(7178)**:583-586.
22. Zhao W, Kruse JP, Tang Y, Jung SY, Qin J, Gu W: **Negative regulation of the deacetylase SIRT1 by DBC1.** *Nature* 2008, **451(7178)**:587-590.
23. Henry LA, Witt DM: **Resveratrol: phytoestrogen effects on reproductive physiology and behavior in female rats.** *Horm Behav* 2002, **41(2)**:220-228.
24. Bowers JL, Tyulmenkov VV, Jernigan SC, Klinge CM: **Resveratrol acts as a mixed agonist/antagonist for estrogen receptors alpha and beta.** *Endocrinology* 2000, **141(10)**:3657-3667.
25. Gehm BD, McAndrews JM, Chien PY, Jameson JL: **Resveratrol, a polyphenolic compound found in grapes and wine, is an agonist for the estrogen receptor.** *Proc Natl Acad Sci USA* 1997, **94(25)**:14138-14143.
26. Singh UP, Singh NP, Singh B, Hofseth LJ, Price RL, Nagarkatti M, Nagarkatti PS: **Resveratrol (trans-3,5,4'-trihydroxystilbene) induces silent mating type information regulation-1 and down-regulates nuclear transcription factor-kappaB activation to abrogate dextran sulfate sodium-induced colitis.** *J Pharmacol Exp Ther* 2010, **332(3)**:829-839.
27. Hou X, Xu S, Maitland-Toolan KA, Sato K, Jiang B, Ido Y, Lan F, Walsh K, Wierzbicki M, Verbeuren TJ, *et al*: **SIRT1 regulates hepatocyte lipid metabolism through activating AMP-activated protein kinase.** *J Biol Chem* 2008, **283(29)**:20015-20026.
28. Suchankova G, Nelson LE, Gerhart-Hines Z, Kelly M, Gauthier MS, Saha AK, Ido Y, Puigserver P, Ruderman NB: **Concurrent regulation of AMP-activated protein kinase and SIRT1 in mammalian cells.** *Biochem Biophys Res Commun* 2009, **378(4)**:836-841.
29. Um JH, Park SJ, Kang H, Yang S, Foretz M, McBurney MW, Kim MK, Viollet B, Chung JH: **AMP-activated protein kinase-deficient mice are resistant to the metabolic effects of resveratrol.** *Diabetes* 2010, **59(3)**:554-563.
30. Chung S, Yao H, Caito S, Hwang JW, Arunachalam G, Rahman I: **Regulation of SIRT1 in cellular functions: role of polyphenols.** *Arch Biochem Biophys* 2010, **501(1)**:79-90.
31. Ragione FD, Cucciolla V, Borriello A, Pietra VD, Racioppi L, Soldati G, Manna C, Galletti P, Zappia V: **Resveratrol arrests the cell division cycle at S/G2 phase transition.** *Biochem Biophys Res Commun* 1998, **250(1)**:53-58.
32. Minegishi T, Tano M, Abe Y, Nakamura K, Ibuki Y, Miyamoto K: **Expression of luteinizing hormone/human chorionic gonadotrophin (LH/HCG) receptor mRNA in the human ovary.** *Mol Hum Reprod* 1997, **3(2)**:101-107.
33. Devoto L, Kohen P, Vega M, Castro O, Gonzalez RR, Retamales I, Carvallo P, Christenson LK, Strauss JF: **Control of human luteal steroidogenesis.** *Mol Cell Endocrinol* 2002, **186(2)**:137-141.
34. Kiriakidou M, McAllister JM, Sugawara T, Strauss JF: **Expression of steroidogenic acute regulatory protein (StAR) in the human ovary.** *J Clin Endocrinol Metab* 1996, **81(11)**:4122-4128.
35. Devoto L, Kohen P, Munoz A, Strauss JF: **Human corpus luteum physiology and the luteal-phase dysfunction associated with ovarian stimulation.** *Reprod Biomed Online* 2009, **18(Suppl 2)**:19-24.
36. Jurisicova A, Taniuchi A, Li H, Shang Y, Antenos M, Detmar J, Xu J, Matikainen T, Benito Hernandez A, Nunez G, *et al*: **Maternal exposure to polycyclic aromatic hydrocarbons diminishes murine ovarian reserve via induction of Harakiri.** *J Clin Invest* 2007, **117(12)**:3971-3978.

doi:10.1186/1477-7827-10-14
Cite this article as: Morita *et al.*: Resveratrol promotes expression of SIRT1 and StAR in rat ovarian granulosa cells: an implicative role of SIRT1 in the ovary. *Reproductive Biology and Endocrinology* 2012 **10**:14.

Med Oncol (2012) 29:1255–1257
DOI 10.1007/s12032-011-9893-0

CASE REPORT

Interstitial pneumonitis induced by pegylated liposomal doxorubicin in a patient with recurrent ovarian cancer

Kanako Inaba · Takahide Arimoto · Mari Hoya · Kei Kawana · Shunsuke Nakagawa · Shiro Kozuma · Yuji Taketani

Received: 24 February 2011 / Accepted: 28 February 2011 / Published online: 10 March 2011

Abstract Interstitial pneumonitis after treatment with pegylated liposomal doxorubicin (PLD) has been rarely reported. We describe herein a case of interstitial pneumonitis in a 49-year-old woman with relapsed ovarian carcinoma treated with PLD. Twenty-five days after the second administration of PLD, she presented with fever and dry cough, and chest CT scans revealed bilateral interstitial infiltrates and ground-glass opacities. She was diagnosed to have interstitial pneumonitis induced by PLD. Steroid therapy improved her symptoms.

Keywords Interstitial pneumonitis · Pegylated liposomal doxorubicin · Drug induced · Japanese · Ovarian cancer

Introduction

Pegylated liposomal doxorubicin (PLD) is an active drug in recurrent ovarian cancer as demonstrated in trials in the second-line chemotherapy [1–3]. It has been designed to enhance the efficacy and to reduce the toxicities of doxorubicin such as cardiotoxicity, hematologic toxicity, and alopecia by using a unique delivery system: a polyethylene glycol coat [4, 5]. Whereas hand-foot syndrome and planter palmar erythema are widely recognized as adverse effects of PLD, few cases of interstitial pneumonitis after treatment with PLD have been reported. Here, we describe a case of interstitial pneumonitis induced by PLD.

K. Inaba · T. Arimoto (✉) · M. Hoya · K. Kawana · S. Nakagawa · S. Kozuma · Y. Taketani
Department of Obstetrics and Gynecology, Faculty of Medicine, The University of Tokyo, 7-3-1 Hongo, Bunkyo-ku, Tokyo 113-8655, Japan
e-mail: tarimoto-tky@umin.ac.jp

Case report

A 48-year-old woman (gravida 4, para 3) with recurrent ovarian cancer was started on third-line chemotherapy with PLD (50 mg/m^2/4 weeks). She was initially diagnosed in February 2009 and underwent complete debulking surgery for a stage IIIC serous ovarian adenocarcinoma. Postoperatively, she received adjuvant chemotherapy with six cycles of paclitaxel (175 mg/m^2) and carboplatin (AUC 6). Four months later, because of peritoneum dissemination and elevation of CA125, she was treated with weekly CPT-11 (95 mg/m^2/week) with progressive disease after four cycles. In April 2010, PLD was given under her excellent performance status.

Twenty-three days after the first administration of PLD, she developed a fever from which she recovered without any treatment. However, 25 days after the second administration of PLD, she presented to our hospital with fever, chill, dry cough, and dyspnea (grade 3 according to Common terminology criteria for adverse events, version 4.0). Physical examination was remarkable for bilateral fine crackles at the lung bases. A chest X-ray and chest CT scans revealed bilateral interstitial infiltrates and ground-glass opacities, though chest CT scans performed before PLD therapy showed clear lung field (Fig. 1a, b). Oxygen saturation by pulse oximetry was 89% on room air and arterial blood gas analysis showed hypoxia (FiO_2 0.32, PaO_2 90.5 mmHg, alveolar-arterial oxygen gradient 94.9 mmHg). Laboratory analysis revealed white blood cells of 2,500/μl with 78% neutrophils, lactate dehydrogenase of 347 IU/l, C-reactive protein of 14.32 mg/dl, and Krebs von den Lungen-6 (KL-6) of 227 U/ml.

Her clinical course and laboratory data indicated that she has interstitial pneumonitis probably induced by PLD. She had not received granulocyte colony-stimulating